

Accurate De Novo Prediction of Protein Contact Map by Ultra-Deep Learning Model

Sheng Wang, Siqu Sun, Zhen Li, Renyu Zhang and Jinbo Xu*

Toyota Technological Institute at Chicago

jinboxu@gmail.com

*: corresponding author

The first two authors contribute equally

Abstract

Motivation: Protein contacts contain key information for the understanding of protein structure and function and thus, contact prediction from sequence is an important problem. Recently exciting progress has been made on this problem, but the predicted contacts for proteins without many sequence homologs is still of low quality and not extremely useful for de novo structure prediction.

Method: This paper presents a new deep learning method that predicts contacts by integrating both evolutionary coupling (EC) and sequence conservation information through an ultra-deep neural network formed by two deep residual neural networks. The first residual network conducts a series of 1-dimensional convolutional transformation of sequential features; the second residual network conducts a series of 2-dimensional convolutional transformation of pairwise information including output of the first residual network, EC information and pairwise potential. By using very deep residual networks, we can accurately model contact occurring patterns and complex sequence-structure relationship and thus, obtain high-quality contact prediction regardless of how many sequence homologs are available for proteins in question.

Results: Our method greatly outperforms existing methods and leads to much more accurate contact-assisted folding. Tested on 105 CASP11 targets, 76 past CAMEO hard targets, and 398 membrane proteins, the average top L long-range prediction accuracy obtained our method, one representative EC method CCMpred and the CASP11 winner MetaPSICOV is 0.47, 0.21 and 0.30, respectively; the average top L/10 long-range accuracy of our method, CCMpred and MetaPSICOV is 0.77, 0.47 and 0.59, respectively. Ab initio folding using our predicted contacts as restraints **but without any force fields** can yield correct folds (i.e., TMscore>0.6) for 203 of the 579 test proteins, while that using MetaPSICOV- and CCMpred-predicted contacts can do so for only 79 and 62 of them, respectively. Our contact-assisted models also have much better quality than template-based models especially for membrane proteins. The 3D models built from our contact prediction have TMscore>0.5 for 208 of the 398 membrane proteins, while those from homology modeling have TMscore>0.5 for

34 only 10 of them. Further, even if trained by only non-membrane proteins, our deep learning method
35 works very well on membrane protein contact prediction. In the recent blind CAMEO benchmark, our
36 fully-automated web server implementing this method successfully folded 5 targets with a new fold and
37 only 0.3L-2.3L effective sequence homologs, including one β protein of 182 residues, one $\alpha+\beta$ protein
38 of 125 residues, one α protein of 140 residues, one α protein of 217 residues and one α/β of 260
39 residues.

40 **Availability:** <http://raptorx.uchicago.edu/ContactMap/>

41 Author Summary

42 Protein contact prediction and contact-assisted folding has made good progress due to direct
43 evolutionary coupling analysis (DCA). However, DCA is effective on only some proteins with a very
44 large number of sequence homologs. To further improve contact prediction, we borrow ideas from deep
45 learning, which has recently revolutionized object recognition, speech recognition and the GO game.
46 Our deep learning method can model complex sequence-structure relationship and high-order
47 correlation (i.e., contact occurring patterns) and thus, improve contact prediction accuracy greatly. Our
48 test results show that our method greatly outperforms the state-of-the-art methods regardless how many
49 sequence homologs are available for a protein in question. Ab initio folding guided by our predicted
50 contacts may fold many more test proteins than the other contact predictors. Our contact-assisted 3D
51 models also have much better quality than homology models built from the training proteins, especially
52 for membrane proteins. One interesting finding is that even trained with only soluble proteins, our
53 method performs very well on membrane proteins. Recent blind test in CAMEO confirms that our
54 method can fold large proteins with a new fold and only a small number of sequence homologs.

55 Introduction

56 De novo protein structure prediction from sequence alone is one of most challenging problems in
57 computational biology. Recent progress has indicated that some correctly-predicted long-range contacts
58 may allow accurate topology-level structure modeling (1) and that direct evolutionary coupling
59 analysis (DCA) of multiple sequence alignment (MSA) may reveal some long-range native contacts for
60 proteins and protein-protein interactions with a large number of sequence homologs (2, 3). Therefore,
61 contact prediction and contact-assisted protein folding has recently gained much attention in the
62 community. However, for many proteins especially those without many sequence homologs, the
63 predicted contacts by the state-of-the-art predictors such as CCMpred (4), PSICOV (5), Evfold (6),
64 plmDCA(7), Gremlin(8), MetaPSICOV (9) and CoinDCA (10) are still of low quality and insufficient
65 for accurate contact-assisted protein folding (11,12). This motivates us to develop a better contact
66 prediction method, especially for proteins without a large number of sequence homologs. In this paper
67 we define that two residues form a contact if they are spatially proximal in the native structure, i.e., the
68 Euclidean distance of their C_{β} atoms less than 8\AA (13).

69 Existing contact prediction methods roughly belong to two categories: evolutionary coupling analysis

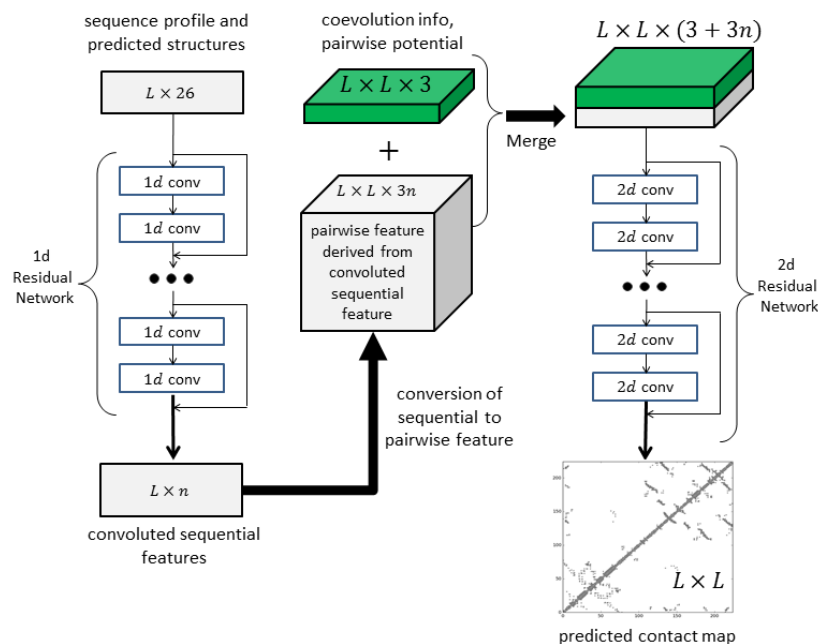
70 (ECA) and supervised machine learning. ECA predicts contacts by identifying co-evolved residues in a
71 protein, such as EVfold (6), PSICOV (5), CCMpred (4), Gremlin (8), plmDCA and others (14-16).
72 However, DCA usually needs a large number of sequence homologs to be effective (10, 17).
73 Supervised machine learning predicts contacts from a variety of information, e.g., SVMSEQ (18),
74 CMAPpro (13), PconsC2 (17), MetaPSICOV (9), PhyCMAP (19) and CoinDCA-NN (10). Meanwhile,
75 PconsC2 uses a 5-layer supervised learning architecture (17); CoinDCA-NN and MetaPSICOV employ
76 a 2-layer neural network (9). CMAPpro uses a neural network with more layers, but its performance
77 saturates at about 10 layers. Some supervised methods such as MetaPSICOV and CoinDCA-NN
78 outperform ECA on proteins without many sequence homologs, but their performance is still limited by
79 their shallow architectures.

80 To further improve supervised learning methods for contact prediction, we borrow ideas from very
81 recent breakthrough in computer vision. In particular, we have greatly improved contact prediction by
82 developing a brand-new deep learning model called residual neural network (20) for contact prediction.
83 Deep learning is a powerful machine learning technique that has revolutionized image classification
84 (21, 22) and speech recognition (23). In 2015, ultra-deep residual neural networks (24) demonstrated
85 superior performance in several computer vision challenges (similar to CASP) such as image
86 classification and object recognition (25). If we treat a protein contact map as an image, then protein
87 contact prediction is kind of similar to (but not exactly same as) pixel-level image labeling, so some
88 techniques effective for image labeling may also work for contact prediction. However, there are some
89 important differences between image labeling and contact prediction. First, in computer vision
90 community, image-level labeling (i.e., classification of a single image) has been extensively studied,
91 but there are much fewer studies on pixel-level image labeling (i.e., classification of an individual
92 pixel). Second, in many image classification scenarios, image size is resized to a fixed value, but we
93 cannot resize a contact map since we need to do prediction for every residue pair (equivalent to an
94 image pixel). Third, contact prediction has much more complex input features (including both
95 sequential and pairwise features) than image labeling. Fourth, the ratio of contacts in a protein is very
96 small (<2%). That is, the number of positive and negative labels in contact prediction is extremely
97 unbalanced.

98 In this paper we present a very deep residual neural network for contact prediction. Such a network can
99 capture very complex sequence-contact relationship and high-order contact correlation. We train this
100 deep neural network using a subset of proteins with solved structures and then test its performance on
101 public data including the CASP (26, 27) and CAMEO (28) targets as well as many membrane proteins.
102 Our experimental results show that our method yields much better accuracy than existing methods and
103 also result in much more accurate contact-assisted folding. The deep learning method described here
104 will also be useful for the prediction of protein-protein and protein-RNA interfacial contacts.

105 Results

106 Deep learning model for contact prediction



107

108 **Figure 1.** Illustration of our deep learning model for contact prediction. Meanwhile, L is the sequence
 109 length of one protein under prediction.

110 Fig. 1 illustrates our deep neural network model for contact prediction (29). Different from previous
 111 supervised learning approaches(9, 13) for contact prediction that employ only a small number of
 112 hidden layers (i.e., a shallow architecture), our deep neural network employs dozens of hidden layers.
 113 By using a very deep architecture, our model can automatically learn the complex relationship between
 114 sequence information and contacts and also model the interdependency among contacts and thus,
 115 improve contact prediction (17). Our model consists of two major modules, each being a residual
 116 neural network. The first module conducts a series of 1-dimensional (1D) convolutional
 117 transformations of sequential features (sequence profile, predicted secondary structure and solvent
 118 accessibility). The output of this 1D convolutional network is converted to a 2-dimensional (2D)
 119 matrix by an operation similar to outer product and then fed into the 2nd module together with pairwise
 120 features (i.e., co-evolution information, pairwise contact and distance potential). The 2nd module is a
 121 2D residual network that conducts a series of 2D convolutional transformations of its input. Finally,
 122 the output of the 2D convolutional network is fed into a logistic regression, which predicts the probability
 123 of any two residues form a contact. In addition, each convolutional layer is also preceded by a simple
 124 nonlinear transformation called rectified linear unit (30). **Mathematically, the output of 1D residual**
 125 **network is just a 2D matrix with dimension $L \times m$ where m is the number of new features (or hidden**
 126 **neurons) generated by the last convolutional layer of the network. Biologically, this 1D residual**
 127 **network learns the sequential context of a residue. By stacking multiple convolution layers, the**

128 network can learn information in a very large sequential context. The output of a 2D convolutional
 129 layer has dimension $L \times L \times n$ where n is the number of new features (or hidden neurons) generated by
 130 this layer for one residue pair. The 2D residual network mainly learns contact occurring patterns or
 131 high-order residue correlation (i.e., 2D context of a residue pair). The number of hidden neurons may
 132 vary at each layer.

133 Our test data includes the 150 Pfam families described in (5), 105 CASP11 test proteins (31), 398
 134 membrane proteins (Supplementary Table 1) and 76 CAMEO hard targets released from 10/17/2015 to
 135 04/09/2016 (Supplementary Table 2). The tested methods include PSICOV (5), Evfold (6), CCMpred
 136 (4), plmDCA(7), Gremlin(8), and MetaPSICOV (9). The former 5 methods employs pure DCA while
 137 MetaPSICOV (9) is a supervised learning method that performed the best in CASP11 (31). All the
 138 programs are run with parameters set according to their respective papers. We cannot evaluate PconsC2
 139 (17) since we failed to obtain any results from its web server. PconsC2 did not outperform
 140 MetaPSICOV in CASP11 (31), so it may suffice to just compare our method with MetaPSICOV.

141 Overall Performance

142 We evaluate the accuracy of the top L/k ($k=10, 5, 2, 1$) predicted contacts where L is protein sequence
 143 length (10). We define that a contact is short-, medium- and long-range when the sequence distance of
 144 the two residues in a contact falls into $[6, 11]$, $[12, 23]$, and ≥ 24 , respectively. The prediction
 145 accuracy is defined as the percentage of native contacts among the top L/k predicted contacts. When
 146 there are no L/k native (short- or medium-range) contacts, we replace the denominator by L/k in
 147 calculating accuracy. This may make the short- and medium-range accuracy look small although it is
 148 easier to predict short- and medium-range contacts than long-range ones.

149 **Table 1.** Contact prediction accuracy on the 150 Pfam families.

Method	Short				Medium				Long			
	L/10	L/5	L/2	L	L/10	L/5	L/2	L	L/10	L/5	L/2	L
EVfold	0.50	0.40	0.26	0.17	0.64	0.52	0.34	0.22	0.74	0.68	0.53	0.39
PSICOV	0.58	0.43	0.26	0.17	0.65	0.51	0.32	0.20	0.77	0.70	0.52	0.37
CCMpred	0.65	0.50	0.29	0.19	0.73	0.60	0.37	0.23	0.82	0.76	0.62	0.45
plmDCA	0.66	0.50	0.29	0.19	0.72	0.60	0.36	0.22	0.81	0.76	0.61	0.44
Gremlin	0.66	0.51	0.30	0.19	0.74	0.60	0.37	0.23	0.82	0.76	0.63	0.46
MetaPSICOV	0.82	0.70	0.45	0.27	0.83	0.73	0.52	0.33	0.92	0.87	0.74	0.58
Our method	0.93	0.81	0.51	0.30	0.93	0.86	0.62	0.38	0.98	0.96	0.89	0.74

150 **Table 2.** Contact prediction accuracy on 105 CASP11 test proteins.

Method	Short				Medium				Long			
	L/10	L/5	L/2	L	L/10	L/5	L/2	L	L/10	L/5	L/2	L
EVfold	0.25	0.21	0.15	0.12	0.33	0.27	0.19	0.13	0.37	0.33	0.25	0.19
PSICOV	0.29	0.23	0.15	0.12	0.34	0.27	0.18	0.13	0.38	0.33	0.25	0.19

CCMpred	0.35	0.28	0.17	0.12	0.40	0.32	0.21	0.14	0.43	0.39	0.31	0.23
plmDCA	0.32	0.26	0.17	0.12	0.39	0.31	0.21	0.14	0.42	0.38	0.30	0.23
Gremlin	0.35	0.27	0.17	0.12	0.40	0.31	0.21	0.14	0.44	0.40	0.31	0.23
MetaPSICOV	0.69	0.58	0.39	0.25	0.69	0.59	0.42	0.28	0.60	0.54	0.45	0.35
Our method	0.82	0.70	0.46	0.28	0.85	0.76	0.55	0.35	0.81	0.77	0.68	0.55

151

Table 3. Contact prediction accuracy on 76 past CAMEO hard targets.

Method	Short				Medium				Long			
	L/10	L/5	L/2	L	L/10	L/5	L/2	L	L/10	L/5	L/2	L
EVfold	0.17	0.13	0.11	0.09	0.23	0.19	0.13	0.10	0.25	0.22	0.17	0.13
PSICOV	0.20	0.15	0.11	0.08	0.24	0.19	0.13	0.09	0.25	0.23	0.18	0.13
CCMpred	0.22	0.16	0.11	0.09	0.27	0.22	0.14	0.10	0.30	0.26	0.20	0.15
plmDCA	0.23	0.18	0.12	0.09	0.27	0.22	0.14	0.10	0.30	0.26	0.20	0.15
Gremlin	0.21	0.17	0.11	0.08	0.27	0.22	0.14	0.10	0.31	0.26	0.20	0.15
MetaPSICOV	0.56	0.47	0.31	0.20	0.53	0.45	0.32	0.22	0.47	0.42	0.33	0.25
Our method	0.67	0.57	0.37	0.23	0.69	0.61	0.42	0.28	0.69	0.65	0.55	0.42

152

Table 4. Contact prediction accuracy on 398 membrane proteins.

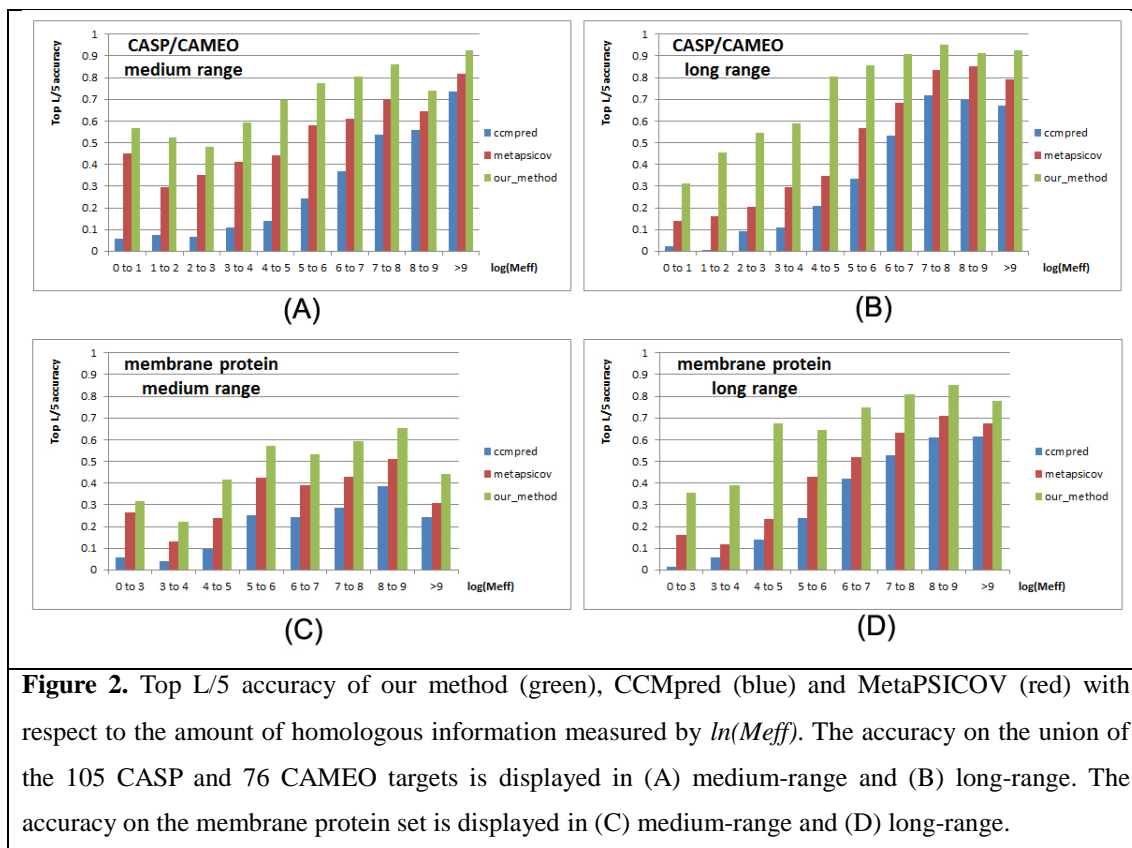
Method	Short				Medium				Long			
	L/10	L/5	L/2	L	L/10	L/5	L/2	L	L/10	L/5	L/2	L
EVfold	0.16	0.13	0.09	0.07	0.28	0.22	0.13	0.09	0.44	0.37	0.26	0.18
PSICOV	0.22	0.16	0.10	0.07	0.29	0.21	0.13	0.09	0.42	0.34	0.23	0.16
CCMpred	0.27	0.19	0.11	0.08	0.36	0.26	0.15	0.10	0.52	0.45	0.31	0.21
plmDCA	0.26	0.18	0.11	0.08	0.35	0.25	0.14	0.09	0.51	0.42	0.29	0.20
Gremlin	0.27	0.19	0.11	0.07	0.37	0.26	0.15	0.10	0.52	0.45	0.32	0.21
MetaPSICOV	0.45	0.35	0.22	0.14	0.49	0.40	0.27	0.18	0.61	0.55	0.42	0.30
Our method	0.60	0.46	0.27	0.16	0.66	0.53	0.33	0.22	0.78	0.73	0.62	0.47

153

154 As shown in Tables 1-4, our method outperforms all tested DCA methods and MetaPSICOV by a very
 155 large margin on the 4 test sets regardless of how many top predicted contacts are evaluated and no
 156 matter whether the contacts are short-, medium- or long-range. These results also show that two
 157 supervised learning methods greatly outperform the pure DCA methods and the three
 158 pseudo-likelihood DCA methods plmDCA, Gremlin and CCMpred perform similarly, but outperform
 159 PSICOV (Gaussian model) and Evfold (maximum-entropy method). The advantage of our method is
 160 the smallest on the 150 Pfam families because many of them have a pretty large number of sequence
 161 homologs. In terms of top L long-range contact accuracy on the CASP11 set, our method exceeds
 162 CCMpred and MetaPSICOV by 0.32 and 0.20, respectively. On the 76 CAMEO hard targets, our
 163 method exceeds CCMpred and MetaPSICOV by 0.27 and 0.17, respectively. On the 398 membrane

164 protein set, our method exceeds CCMpred and MetaPSICOV by 0.26 and 0.17, respectively. Our
 165 method uses a subset of protein features used by MetaPSICOV, but performs much better than
 166 MetaPSICOV due to our deep architecture and that we predict contacts of a protein simultaneously.
 167 Since the Pfam set is relatively easy, we will not analyze it any more in the following sections.

168 Prediction accuracy with respect to the number of sequence homologs



169 To examine the performance of our method with respect to the amount of homologous information
 170 available for a protein under prediction, we measure the effective number of sequence homologs in
 171 multiple sequence alignment (MSA) by $Meff$ (19), which can be roughly interpreted as the number of
 172 non-redundant sequence homologs when 70% sequence identity is used as cutoff to remove
 173 redundancy (see Method for its formula). A protein with a smaller $Meff$ has less homologous
 174 information. We divide all the test proteins into 10 bins according to $\ln(Meff)$ and then calculate the
 175 average accuracy of proteins in each bin. We merge the first 3 bins for the membrane protein set since
 176 they have a small number of proteins.

177 Fig. 2 shows that the top L/5 contact prediction accuracy increases with respect to $Meff$, i.e., the
 178 number of effective sequence homologs, and that our method outperforms both MetaPSICOV and
 179 CCMpred regardless of $Meff$. Our long-range prediction accuracy is even better when $\ln(Meff) \leq 7$
 180 (equivalently $Meff < 1100$), i.e., when the protein under prediction does not have a very large number of
 181 non-redundant sequence homologs. Our method has a large advantage over the other methods even
 182 when $Meff$ is very big (>8000). This indicates that our method indeed benefits from some extra

183 information such as inter-contact correlation or high-order residue correlation, which is orthogonal to
184 pairwise co-evolution information.

185 Contact-assisted protein folding

186 One of the important goals of contact prediction is to perform contact-assisted protein folding (11). To
187 test if our contact prediction can lead to better 3D structure modeling than the others, we build structure
188 models for all the test proteins using the top predicted contacts as restraints of ab initio folding. For
189 each test protein, we feed the top predicted contacts as restraints into the CNS suite (32) to generate 3D
190 models. We measure the quality of a 3D model by a superposition-dependent score TMscore (33) ,
191 which ranges from 0 to 1, with 0 indicating the worst and 1 the best, respectively. We also measure the
192 quality of a 3D model by a superposition-independent score IDDT, which ranges from 0 to 100, with 0
193 indicating the worst and 100 the best, respectively.

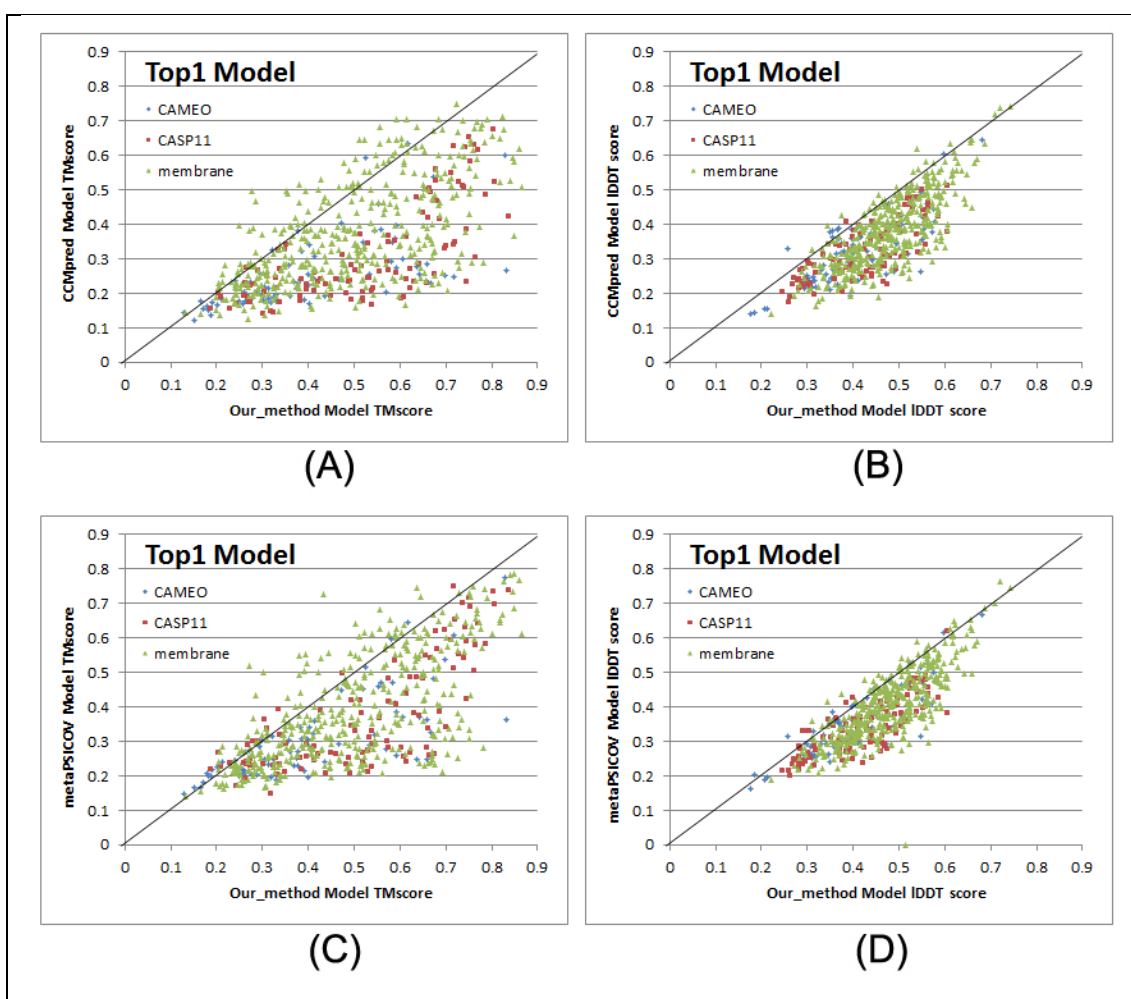


Figure 3. Quality comparison of top 1 contact-assisted models generated by our method, CCMpred and MetaPSICOV on the 105 CASP11 targets (red square), 76 CAMEO targets (blue diamond) and 398 membrane protein targets (green triangle), respectively. (A) and (B): comparison between our method (X-axis) and CCMpred (Y-axis) in terms of TMscore and IDDT, respectively. (C) and (D): comparison between our method (X-axis) and MetaPSICOV (Y-axis) in terms of TMscore and IDDT, respectively.

IDDT is scaled to between 0 and 1.

194 Fig. 3 shows that our predicted contacts can generate much better 3D models than CCMpred and
195 MetaPSICOV. On average, our 3D models are better than MetaPSICOV and CCMpred by ~0.12
196 TMsore unit and ~0.15 unit, respectively. When the top 1 models are evaluated, the average TMsore
197 obtained by CCMpred, MetaPSICOV, and our method is 0.333, 0.377, and 0.518, respectively on the
198 CASP dataset. The average IDDT of CCMpred, MetaPSICOV and our method is 31.7, 34.1 and 41.8,
199 respectively. On the 76 CAMEO targets, the average TMsore of CCMpred, MetaPSICOV and our
200 method is 0.256, 0.305 and 0.407, respectively. The average IDDT of CCMpred, MetaPSICOV and our
201 method is 31.8, 35.4 and 40.2, respectively. On the membrane protein set, the average TMsore of
202 CCMpred, MetaPSICOV and our method is 0.354, 0.387, and 0.493, respectively. The average IDDT
203 of CCMpred, MetaPSICOV and our method is 38.1, 40.5 and 47.8, respectively. Same trend is
204 observed when the best of top 5 models are evaluated (Supplementary Figure 1). On the CASP set, the
205 average TMsore of the models generated by CCMpred, MetaPSICOV, and our method is 0.352, 0.399,
206 and 0.543, respectively. The average IDDT of CCMpred, MetaPSICOV and our method is 32.3, 34.9
207 and 42.4, respectively. On the 76 CAMEO proteins, the average TMsore of CCMpred, MetaPSICOV,
208 and our method is 0.271, 0.334, and 0.431, respectively. The average IDDT of CCMpred,
209 MetaPSICOV and our method is 32.4, 36.1 and 40.9, respectively. On the membrane protein set, the
210 average TMsore of CCMpred, MetaPSICOV, and our method is 0.385, 0.417, and 0.516, respectively.
211 The average IDDT of CCMpred, MetaPSICOV and our method is 38.9, 41.2 and 48.5, respectively. In
212 particular, when the best of top 5 models are considered, our predicted contacts can result in correct
213 folds (i.e., TMsore>0.6) for 203 of the 579 test proteins, while MetaPSICOV- and CCMpred-predicted
214 contacts can do so for only 79 and 62 of them, respectively.

215 Our method also generates much better contact-assisted models for the test proteins without many
216 non-redundant sequence homologs. When the 219 of 579 test proteins with $M_{eff} \leq 500$ are evaluated, the
217 average TMsore of the top 1 models generated by our predicted contacts for the CASP11, CAMEO
218 and membrane sets is 0.426, 0.365, and 0.397, respectively. By contrast, the average TMsore of the
219 top 1 models generated by CCMpred-predicted contacts for the CASP11, CAMEO and membrane sets
220 is 0.236, 0.214, and 0.241, respectively. The average TMsore of the top 1 models generated by
221 MetaPSICOV-predicted contacts for the CASP11, CAMEO and membrane sets is 0.292, 0.272, and
222 0.274, respectively.

223 **Contact-assisted models vs. template-based models**

224 To compare the quality of our contact-assisted models and template-based models (TBMs), we built
225 TBMs for all the test proteins using our training proteins as candidate templates. To generate TBMs for
226 a test protein, we first run HHblits (with the UniProt20_2016 library) to generate an HMM file for the
227 test protein, then run HHsearch with this HMM file to search for the best templates among the 6767
228 training proteins, and finally run MODELLER to build a TBM from each of the top 5 templates. Fig. 4
229 shows the head-to-head comparison between our top 1 contact-assisted models and the top 1 TBMs on

230 these three test sets in terms of both TMscore and IDDT. The average IDDT of our top 1
231 contact-assisted models is 45.7 while that of top 1 TBMs is only 20.7. When only the first models are
232 evaluated, our contact-assisted models for the 76 CAMEO test proteins have an average TMscore 0.407
233 while the TBMs have an average TMscore 0.317. On the 105 CASP11 test proteins, the average
234 TMscore of our contact-assisted models is 0.518 while that of the TBMs is only 0.393. On the 398
235 membrane proteins, the average TMscore of our contact-assisted models is 0.493 while that of the
236 TBMs is only 0.149. Same trend is observed when top 5 models are compared (see Supplementary
237 Figure 2). The average IDDT of our top 5 contact-assisted models is 46.4 while that of top 5 TBMs is
238 only 24.0. On the 76 CAMEO test proteins, the average TMscore of our contact-assisted models is
239 0.431 while that of the TBMs is only 0.366. On the 105 CASP11 test proteins, the average TMscore of
240 our contact-assisted models is 0.543 while that of the TBMs is only 0.441. On the 398 membrane
241 proteins, the average TMscore of our contact-assisted models is 0.516 while that of the TBMs is only
242 0.187. The low quality of TBMs further confirms that there is little redundancy between our training
243 and test proteins (especially membrane proteins). This also indicates that our deep model does not
244 predict contacts by simply copying from training proteins. That is, our method can predict contacts for
245 a protein with a new fold.

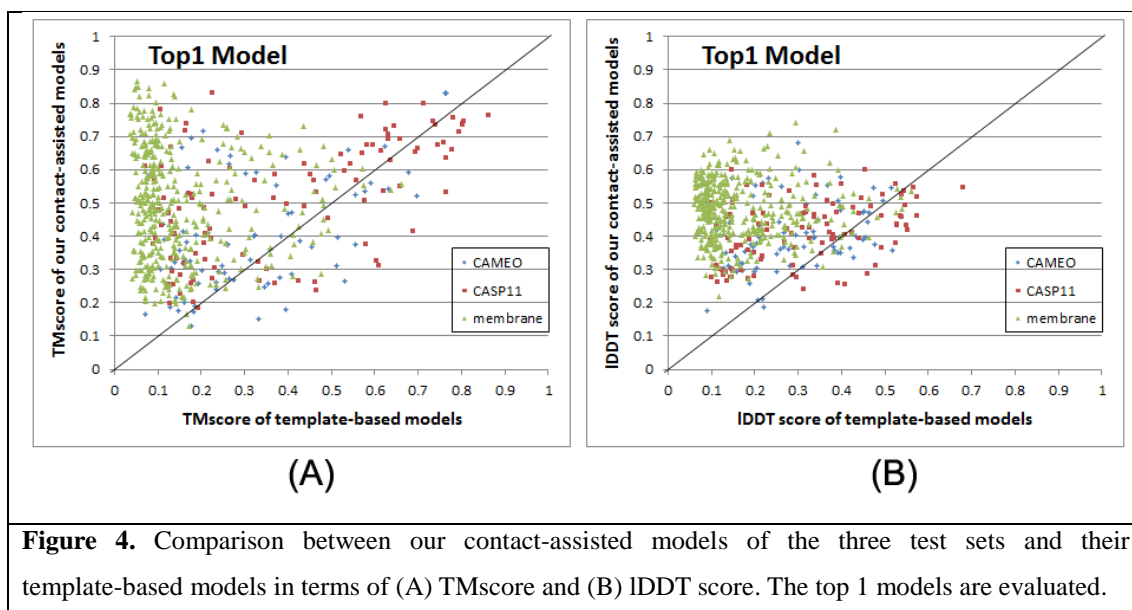


Figure 4. Comparison between our contact-assisted models of the three test sets and their template-based models in terms of (A) TMscore and (B) IDDT score. The top 1 models are evaluated.

246

247 Further, when the best of top 5 models are considered for all the methods, our contact-assisted models
248 have TMscore>0.5 for 24 of the 76 CAMEO targets while TBMs have TMscore>0.5 for only 18 of
249 them. Our contact-assisted models have TMscore >0.5 for 67 of the 105 CASP11 targets while TBMs
250 have TMscore>0.5 for only 44 of them. Our contact-assisted models have TMscore>0.5 for 208 of the
251 398 membrane proteins while TBMs have TMscore >0.5 for only 10 of them. Our contact-assisted
252 models for membrane proteins are much better than their TBMs because there is little similarity
253 between the 6767 training proteins and the 398 test membrane proteins. When the 219 test proteins
254 with ≤ 500 non-redundant sequence homologs are evaluated, the average TMscore of the TBMs is 0.254

255 while that of our contact-assisted models is 0.421. Among these 219 proteins, our contact-assisted
256 models have TMscore>0.5 for 72 of them while TBMs have TMscore>0.5 for only 17 of them.

257 The above results imply that 1) when a query protein has no close templates, our contact-assisted
258 modeling may work better than template-based modeling; 2) contact-assisted modeling shall be
259 particularly useful for membrane proteins; and 3) our deep learning model does not predict contacts by
260 simply copying contacts from the training proteins since our predicted contacts may result in much
261 better 3D models than homology modeling.

262 **Blind test in CAMEO**

263 We have implemented our algorithm as a fully-automated contact prediction web server
264 (<http://raptorx.uchicago.edu/ContactMap/>) and in September 2016 started to blindly test it through the
265 weekly live benchmark CAMEO (<http://www.cameo3d.org/>). CAMEO is operated by the Schwede
266 group, with whom we have never collaborated. CAMEO can be interpreted as a fully-automated CASP,
267 but has a smaller number (>20) of participating servers since many CASP-participating servers are not
268 fully automated and thus, cannot handle the large number of test targets used by CAMEO. Nevertheless,
269 the CAMEO participants include some well-known servers such as Robetta(34), Phyre(35),
270 RaptorX(36), Swiss-Model(37) and HHpred(38). Meanwhile Robetta employs both ab initio folding
271 and template-based modeling while the latter four employ mainly template-based modeling. Every
272 weekend CAMEO sends test sequences to participating servers for prediction and then evaluates 3D
273 models collected from servers. The test proteins used by CAMEO have no publicly available native
274 structures until CAMEO finishes collecting models from participating servers.

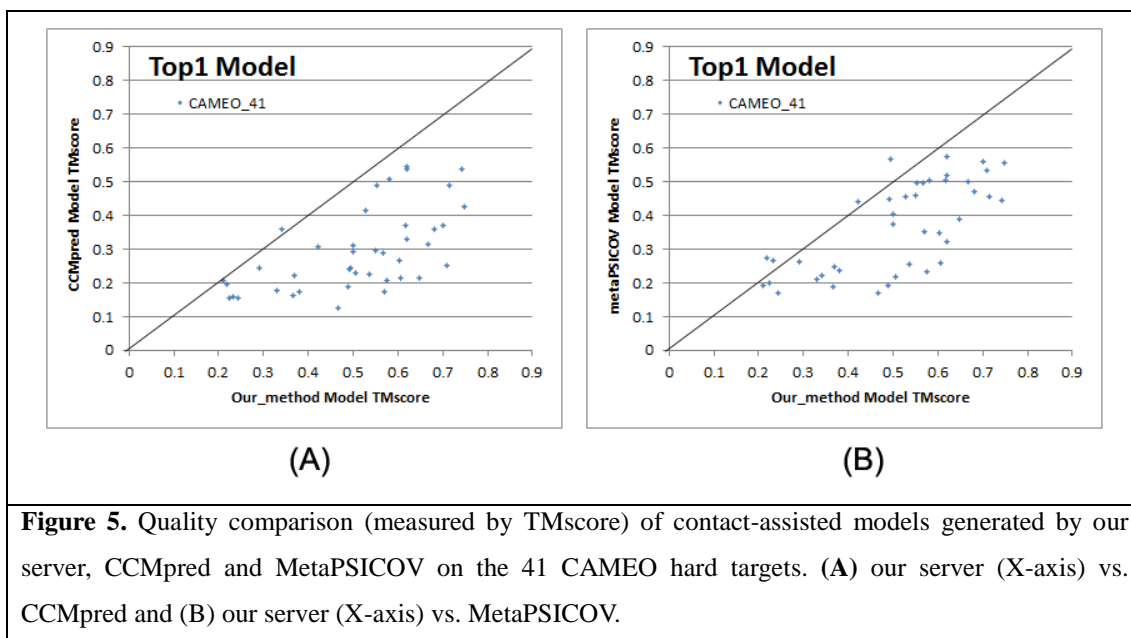
275 During the past 2 months (9/3/2016 to 10/31/2016), CAMEO in total released 41 hard targets
276 (Supplementary Table 3). Although classified as hard by CAMEO, some of them may have
277 distantly-related templates. Table 5 lists the contact prediction accuracy of our server in the blind
278 CAMEO test as compared to the other methods. Again, our method outperforms the others by a very
279 large margin no matter how many contacts are evaluated. The CAMEO evaluation of our
280 contact-assisted 3D models is available at the CAMEO web site. You will need to register CAMEO in
281 order to see all the detailed results of our contact server (ID: server60). Although our server currently
282 build 3D models using only top predicted contacts without any force fields and fragment assembly
283 procedures, our server predicts 3D models with TMscore>0.5 for 28 of the 41 targets and TMscore>0.6
284 for 16 of them. The average TMscore of the best of top 5 models built from the contacts predicted by
285 our server, CCMpred and MetaPSICOV is 0.535, 0.316 and 0.392, respectively. See Fig. 5 for the
286 detailed comparison of the 3D models generated by our server, CCMpred and MetaPSICOV. Our
287 server has also successfully folded 4 targets with a new fold plus one released in November 2016
288 (5flgB). See Table 6 for a summary of our prediction results of these targets and the below subsections
289 for a detailed analysis. Among these targets, 5f5pH is particularly interesting since it has a sequence
290 homolog in PDB but adopting a different conformation. That is, any template-based techniques cannot
291 obtain a good prediction for this target.

292

Table 5. Contact prediction accuracy on 41 recent CAMEO hard targets.

Method	Short				Medium				Long			
	L/10	L/5	L/2	L	L/10	L/5	L/2	L	L/10	L/5	L/2	L
EVfold	0.20	0.15	0.11	0.08	0.25	0.19	0.12	0.09	0.33	0.29	0.21	0.15
PSICOV	0.21	0.16	0.11	0.08	0.26	0.20	0.11	0.08	0.33	0.30	0.21	0.15
plmDCA	0.26	0.19	0.12	0.09	0.28	0.23	0.13	0.09	0.38	0.33	0.24	0.17
Gremlin	0.25	0.18	0.12	0.08	0.29	0.22	0.13	0.09	0.37	0.34	0.25	0.17
CCMpred	0.24	0.18	0.12	0.08	0.29	0.22	0.13	0.09	0.37	0.34	0.24	0.17
MetaPSICOV	0.53	0.43	0.27	0.17	0.51	0.42	0.28	0.19	0.60	0.54	0.40	0.30
Our server	0.67	0.52	0.32	0.20	0.68	0.58	0.38	0.24	0.82	0.75	0.62	0.46

293



294

Table 6. A summary of our blind prediction results on 5 CAMEO hard targets with a new fold.

Target	CAMEO ID	Type	Len	Meff	Method	RMSD(Å)	TMscore
2nc8A	2016-09-10_00000002_1	β	182	250	Our server	6.5	0.61
					Best of the others	12.18	0.47
5dcjA	2016-09-17_00000018_1	$\alpha+\beta$	125	180	Our server	7.9	0.52
					Best of the others	10.0	0.53
5djeB	2016-09-24_00000052_1	α	140	330	Our server	5.81	0.65
					Best of the others	14.98	0.34
5f5pH	2016-10-15_00000047_1	α	217	65	Our server	4.21	0.71

					Best of the others	>40.0	0.48
5flgB	2016-11-12_00000046_1	α/β	260	113	Our server	7.12	0.61
					Best of the others	16.9	0.25

296

297 Among these 41 hard targets, there are five multi-domain proteins: 5idoA, 5hmqF, 5b86B, 5b2gG and
 298 5cylH. Table 7 shows that the average contact prediction accuracy of our method on these 5
 299 multi-domain proteins is much better than the others. For multi-domain proteins, we use a
 300 superposition-independent score IDDT instead of TMscore to measure the quality of a 3D model. As
 301 shown in Table 8, the 3D models built by our server from predicted contacts have much better IDDT
 302 score than those built from CCMpred and MetaPSICOV.

303 **Table 7.** The average contact prediction accuracy of our method and the others on 5 multi-domain
 304 proteins among the 41 CAMEO hard targets.

Method	Short				Medium				Long			
	L/10	L/5	L/2	L	L/10	L/5	L/2	L	L/10	L/5	L/2	L
EVfold	0.17	0.13	0.09	0.07	0.18	0.12	0.08	0.06	0.54	0.40	0.26	0.18
PSICOV	0.27	0.18	0.10	0.07	0.26	0.17	0.11	0.07	0.62	0.49	0.31	0.20
plmDCA	0.29	0.23	0.11	0.07	0.32	0.22	0.11	0.08	0.66	0.51	0.34	0.22
Gremlin	0.30	0.24	0.12	0.08	0.32	0.22	0.12	0.07	0.67	0.52	0.36	0.23
CCMpred	0.30	0.23	0.12	0.08	0.32	0.22	0.12	0.08	0.66	0.51	0.35	0.23
MetaPSICOV	0.52	0.37	0.21	0.14	0.32	0.26	0.16	0.11	0.72	0.58	0.41	0.26
Our method	0.74	0.58	0.33	0.19	0.68	0.55	0.33	0.20	0.96	0.91	0.76	0.57

305

306 **Table 8.** The IDDT score of the 3D models built for the 5 multi-domain proteins using predicted
 307 contacts.

Targets	Length	CCMpred	MetaPSICOV	Our
5idoA	512	23.67	24.24	36.83
5hmqF	637	24.84	25.91	33.16
5b86B	600	29.88	32.85	42.58
5b2gG	364	28.52	30.47	47.91
5cylH	370	22.21	23.37	30.62

308 **Study of CAMEO target 2nc8A (CAMEO ID: 2016-09-10_00000002_1, PDB ID:2nc8)**

309 On September 10, 2016, CAMEO released two hard test targets for structure prediction. Our contact
 310 server successfully folded the hardest one (PDB ID: 2nc8), a mainly β protein of 182 residues. Table 9
 311 shows that our server produced a much better contact prediction than CCMpred and MetaPSICOV.
 312 CCMpred has very low accuracy since HHblits detected only ~250 non-redundant sequence homologs
 313 for this protein, i.e., its $M_{eff}=250$. Fig. 6 shows the predicted contact maps and their overlap with the

314 native. MetaPSICOV fails to predict many long-range contacts while CCMpred introduces too many
315 false positives.

316 **Table 9.** The long- and medium-range contact prediction accuracy of our method, MetaPSICOV and
317 CCMpred on the CAMEO target 2nc8A.

	Long-range accuracy				Medium-range accuracy			
	L	L/2	L/5	L/10	L	L/2	L/5	L/10
Our method	0.764	0.923	0.972	1.0	0.450	0.769	0.972	1.0
MetaPSICOV	0.258	0.374	0.556	0.667	0.390	0.626	0.806	0.944
CCMpred	0.165	0.231	0.389	0.333	0.148	0.187	0.167	0.222

318

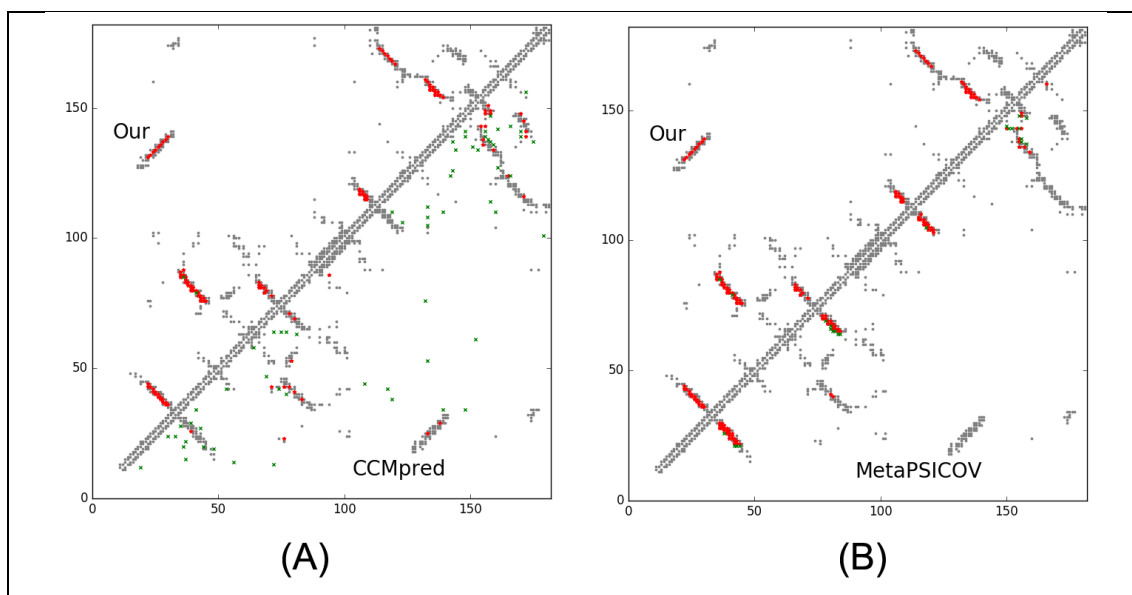


Figure 6. Overlap between top L/2 predicted contacts (in red or green) and the native (in grey). Red (green) dots indicate correct (incorrect) prediction. The left picture shows the comparison between our prediction (in upper-left triangle) and CCMpred (in lower-right triangle) and the right picture shows the comparison between our prediction (in upper-left triangle) and MetaPSICOV (in lower-right triangle).

319

320 The 3D model submitted by our contact server has TMscore 0.570 (As of September 16, 2016, our
321 server submits only one 3D model for each test protein) and the best of our top 5 models has TMscore
322 0.612 and RMSD 6.5Å. Fig. 7 shows that the beta strands of our predicted model (red) matches well
323 with the native (blue). To examine the superimposition of our model with its native structure from
324 various angles, please see <http://raptorx.uchicago.edu/DeepAlign/75097011/>. By contrast, the best of
325 top 5 models built by CNS from CCMpred- and MetaPSICOV-predicted contacts have TMscore 0.206
326 and 0.307, respectively, and RMSD 15.8Å and 14.2Å, respectively. The best TMscore obtained by the
327 other CAMEO-participating servers is only 0.47 (Fig. 8). Three top-notch servers HHpred, RaptorX
328 and Robetta only submitted models with TMscore≤0.30. According to Xu and Zhang (39), a 3D model
329 with TMscore<0.5 is unlikely to have a correct fold while a model with TMscore≥0.6 surely has a

330 correct fold. That is, our contact server predicted a correct fold for this test protein while the others
 331 failed to.

332 This test protein represents almost a novel fold. Our in-house structural homolog search tool
 333 DeepSearch(40) cannot identify structurally very similar proteins in PDB70 (created right before
 334 September 10, 2016) for this test protein. PDB70 is a set of representative structures in PDB, in which
 335 any two share less than 70% sequence identity. DeepSearch
 336 returned two weakly similar proteins 4kx7A and 4g2aA,
 337 which have TMscore 0.521 and 0.535 with the native
 338 structure of the test protein, respectively, and TMscore
 339 0.465 and 0.466 with our best model, respectively. This is
 340 consistent with the fact that none of the template-based
 341 servers in CAMEO submitted a model with TMscore>0.5.
 342 We cannot find structurally similar proteins in PDB70
 343 for our best model either; the best TMscore between PDB70
 344 and our best model is only 0.480. That is, the models
 345 predicted by our method are not simply copied from the
 346 solved structures in PDB, and our method can indeed fold a
 347 relatively large β protein with a novel fold.

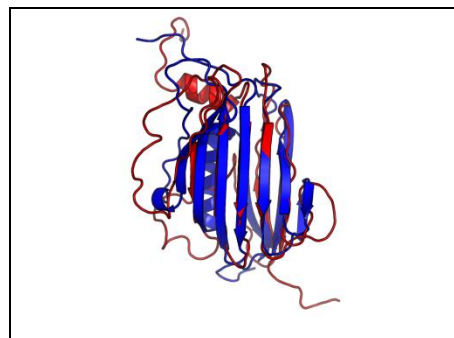


Figure 7. Superimposition between our predicted model (red) and its native structure (blue) for the CAMEO test protein (PDB ID 2nc8 and chain A).

Server Name	Predictions	Resp. time (hh:mm:ss)	From	To	Cov. (%)	IDDT	IDDT Ca	Avg. IDDT-BS	Avg. IDDT-BS details	QScore	QScore details	CAD-Score	GDT_HA	RMSD	GDC	Model Conf.	MaxSub	TMscore
Server 60	Model 1	00:51:19	1	182	100	42.76	50.39	-	-	-	-	0.48	26.46	7.69	36.04	0.50	0.37	0.57
Server 56	Model 1	20:53:42	1	182	100	35.81	43.06	-	-	-	-	0.43	19.88	12.18	27.65	0.80	0.28	0.47
Server 58	Model 1	20:54:33	1	182	100	35.81	43.06	-	-	-	-	0.43	19.88	12.18	27.65	0.80	0.28	0.47
RaptorX	Model 1	01:17:35	1	182	100	28.73	32.74	-	-	-	-	0.41	12.57	17.55	16.32	0.65	0.16	0.30
Server 57	Model 1	20:54:44	1	182	100	28.64	33.07	-	-	-	-	0.39	12.43	13.54	18.68	0.73	0.17	0.36
Server 45	Model 1	01:51:45	1	182	100	28.45	32.88	-	-	-	-	0.43	19.01	21.83	22.86	0.65	0.23	0.36
Robetta	Model 1	51:20:57	10	182	95	28.33	32.62	-	-	-	-	0.45	10.23	25.10	11.51	0.50	0.12	0.21
HHpredB	Model 1	12:14:59	1	182	100	23.70	28.37	-	-	-	-	0.40	12.87	20.72	16.16	0.85	0.17	0.30
Princeton_TEMPLATE	Model 1	01:02:52	1	182	100	23.38	27.09	-	-	-	-	0.38	9.94	23.55	11.52	0.59	0.12	0.24
SPARKS-X	Model 1	00:12:47	1	182	100	23.08	26.26	-	-	-	-	0.37	7.60	19.12	8.89	0.52	0.09	0.20
Server 55	Model 1	00:28:24	1	182	100	22.38	25.78	-	-	-	-	0.39	7.60	23.65	7.81	0.67	0.08	0.20
RBO Aleph	Model 1	65:29:29	1	182	100	21.52	23.78	-	-	-	-	0.35	5.99	20.90	6.86	0.80	0.07	0.17

348 **Figure 8.** The list of CAMEO-participating servers (only 12 of 20 are displayed) and their model
 349 scores. The rightmost column displays the TMscore of submitted models. Server60 is our contact web
 350 server.
 351

352 Study of CAMEO target 5dcjA (CAMEO ID: 2016-09-17_00000018_1, PDB ID:5dcj)

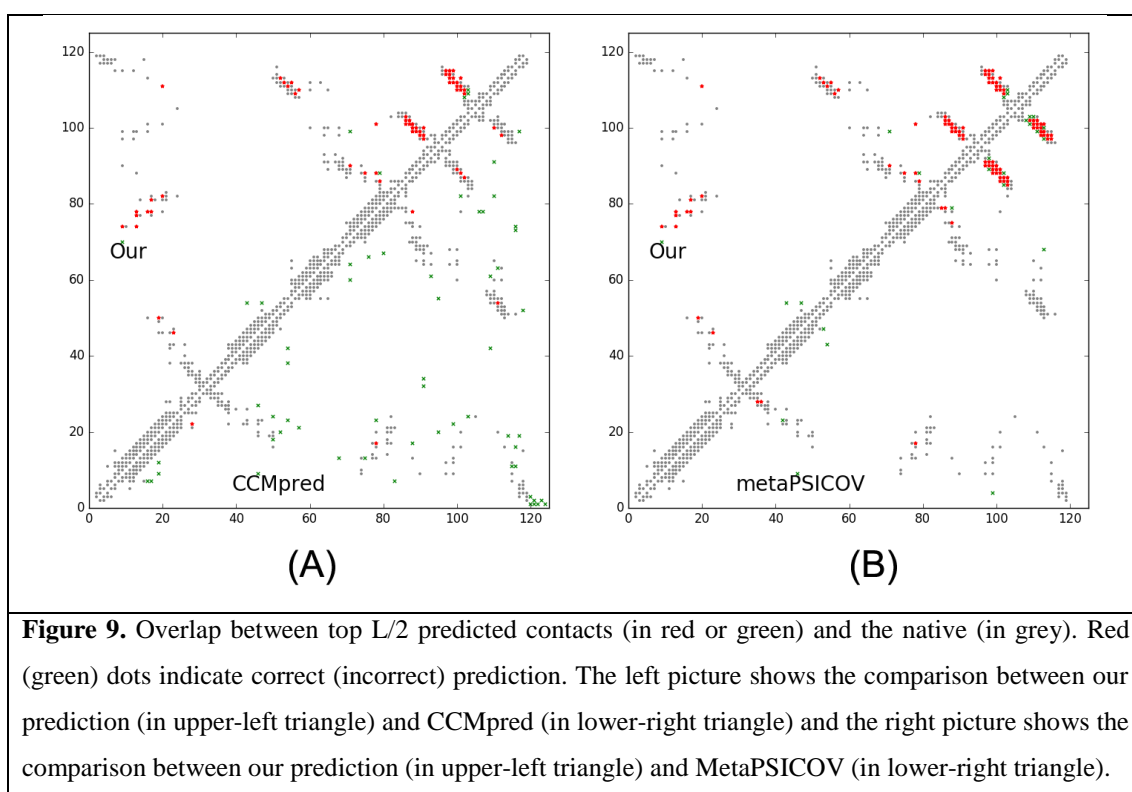
353 This target was released by CAMEO on September 17, 2016. It is an α + β sandwich protein of 125
 354 residues. The four beta sheets of this protein are wrapped by one and three alpha helices at two sides.
 355 Table 10 shows that our server produced a much better contact prediction than CCMpred and
 356 MetaPSICOV. Specifically, the contact map predicted by our method has L/2 long-range accuracy
 357 0.645 while that by CCMpred and MetaPSICOV has L/2 accuracy only 0.05 and 0.194, respectively.

358 CCMpred has very low accuracy since HHblits can only find ~180 non-redundant sequence homologs
 359 for this protein, i.e., its Meff=180. Fig. 9 shows the predicted contact maps and their overlap with the
 360 native. Both CCMpred and metaPSICOV failed to predict some long-range contacts.

361 **Table 10.** The long- and medium-range contact prediction accuracy of our method, MetaPSICOV and
 362 CCMpred on the CAMEO target 5dcjA.

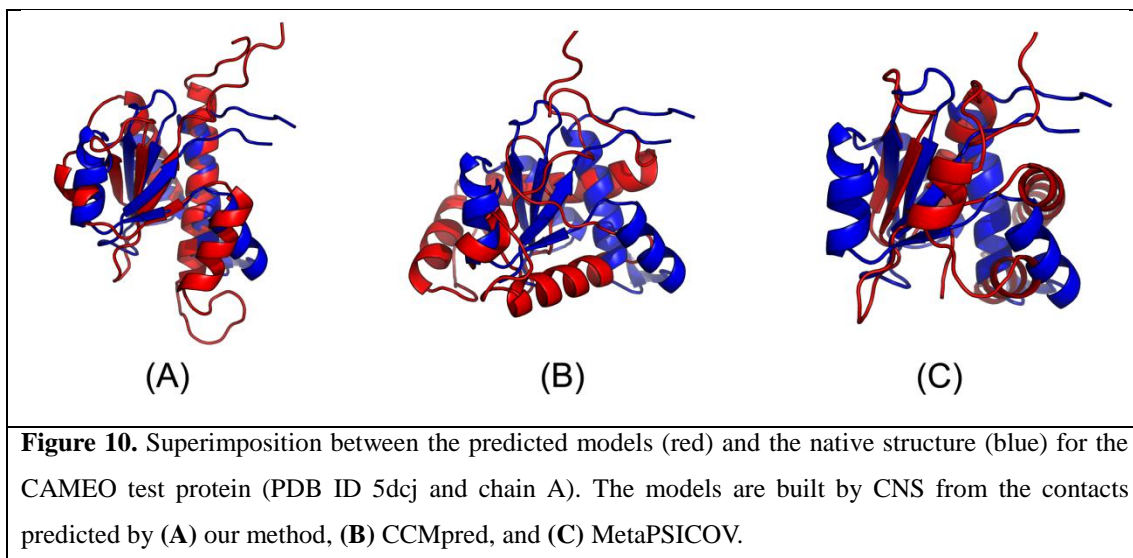
	Long range				Medium range			
	L	L/2	L/5	L/10	L	L/2	L/5	L/10
Our method	0.456	0.645	0.88	0.833	0.36	0.645	0.92	1.0
metaPSICOV	0.144	0.194	0.32	0.25	0.344	0.532	0.8	1.0
CCMpred	0.05	0.05	0.08	0.08	0.1	0.129	0.12	0.25

363



364

365 The first 3D model submitted by our contact server has TMscore 0.50 and the best of our 5 models has
 366 TMscore 0.52 and RMSD 7.9Å. The best of top 5 models built by CNS from CCMpred- and
 367 MetaPSICOV-predicted contacts have TMscore 0.243 and 0.361, respectively. Fig. 10(A) shows that all
 368 the beta strands and the three surrounding alpha helices of our predicted model (in red) matches well
 369 with the native structure (blue), while the models from CCMpred (Fig.10(B)) and MetaPSICOV
 370 (Fig.10(C)) do not have a correct fold. To examine the superimposition of our model with its native
 371 structure from various angles, please see <http://raptorx.uchicago.edu/DeepAlign/92913404/>.



372

373 In terms of TMscore, our models have comparable quality to Robetta, but better than the other servers
 374 (Fig. 11). In terms of IDDT-C α score, our models are better than all the others. In particular, our
 375 method produced better models than the popular homology modeling server HHpredB and our own
 376 template-based modeling server RaptorX, which submitted models with TMscore \leq 0.45.

377 This test protein represents a novel fold. Searching through PDB70 created right before September 17,
 378 2016 by our in-house structural homolog search tool DeepSearch cannot identify structurally similar
 379 proteins for this test protein. The most structurally similar proteins are 3lr5A and 5ereA, which have
 380 TMscore 0.431 and 0.45 with the test protein, respectively. This is consistent with the fact that none of
 381 the template-based servers in CAMEO can predict a good model for this test protein. By contrast, our
 382 contact-assisted model has TMscore 0.52, which is higher than all the template-based models.

Server Name	Predictions	Resp. time (hh:mm:ss)	From	To	Cov (%)	IDDT	IDDT-C α	Avg. IDDT-BS	Avg. IDDT-BS details	QScore	QScore details	CAD-Score	GDT_HA	RMSD	GDC	Model Conf.	MaxSub	TMscore
Server 60	Model 1	11:38:06	1	125	100	47.88	57.13	43.45	CPS1:0.43(1.00)	-	-	0.51	27.97	8.93	32.76	0.50	0.35	0.50
Robetta	Model 1	11:58:59	1	125	100	48.12	54.58	49.79	CPS1:0.50(1.00)	-	-	0.53	29.66	10.39	36.80	0.90	0.41	0.50
Server 56	Model 1	21:07:50	1	125	100	46.12	53.12	39.74	CPS1:0.40(1.00)	-	-	0.51	28.39	10.06	34.81	0.96	0.38	0.48
Server 58	Model 1	21:06:20	1	125	100	46.12	53.12	39.74	CPS1:0.40(1.00)	-	-	0.51	28.39	10.06	34.81	0.96	0.38	0.48
RaptorX	Model 1	10:28:22	1	125	100	45.12	50.42	38.20	CPS1:0.38(1.00)	-	-	0.51	26.91	10.10	32.71	0.65	0.32	0.45
Princeton_TEMPLATE	Model 1	04:55:57	1	125	100	44.32	50.33	37.68	CPS1:0.38(1.00)	-	-	0.47	23.73	10.69	31.45	0.50	0.33	0.45
Server 45	Model 1	10:53:53	1	125	100	44.39	49.91	35.88	CPS1:0.36(1.00)	-	-	0.51	26.70	11.97	33.12	0.64	0.34	0.46
SPARKS-X	Model 1	00:46:54	1	125	100	42.67	49.20	36.24	CPS1:0.36(1.00)	-	-	0.49	25.64	11.71	32.24	0.54	0.33	0.45
HHpredB	Model 1	80:54:59	1	125	100	42.56	48.88	37.32	CPS1:0.37(1.00)	-	-	0.49	26.27	11.62	32.21	0.89	0.33	0.45
Server 55	Model 1	00:08:10	1	125	100	42.14	48.44	36.60	CPS1:0.37(1.00)	-	-	0.50	26.27	10.16	31.85	0.88	0.33	0.45
Server 54	Model 1	00:00:57	3	121	95	42.29	48.43	37.01	CPS1:0.37(1.00)	-	-	0.50	26.48	10.13	31.75	0.89	0.33	0.45
SWISS-MODEL	Model 1	00:01:06	3	121	95	41.93	48.31	34.95	CPS1:0.35(1.00)	-	-	0.49	27.33	10.15	31.78	0.90	0.33	0.45
Server 48	Model 1	00:02:00	3	121	95	41.93	48.31	34.90	CPS1:0.35(1.00)	-	-	0.49	27.33	10.15	31.78	0.90	0.33	0.45
InfOLD3-TS	Model 1	22:08:20	1	125	100	42.67	48.00	38.51	CPS1:0.39(1.00)	-	-	0.47	25.42	11.87	30.96	0.74	0.31	0.44

383

384 **Figure 11.** The list of CAMEO-participating servers (only 14 of 20 are displayed) and their model
 385 scores, sorted by IDDT-C α . The rightmost column displays the TMscore of submitted models. Server60
 386 is our contact web server.

387 **Study of CAMEO target 5djeB (CAMEO ID: 2016-09-24_0000052_1, PDB ID: 5dje)**

388 This target was released on September 24, 2016. It is an alpha protein of 140 residues with a novel fold.
389 Table 11 shows that our server produced a much better contact prediction than CCMpred and
390 MetaPSICOV. Specifically, the contact map predicted by our method has L/5 and L/10 long-range
391 accuracy 50.0% and 71.4%, respectively, while that by CCMpred and MetaPSICOV has L/5 and L/10
392 accuracy less than 30%. CCMpred has low accuracy since HHblits can only find ~330 non-redundant
393 sequence homologs for this protein, i.e., its $M_{eff}=330$. Fig. 12 shows the predicted contact maps and
394 their overlap with the native. Both CCMpred and metaPSICOV failed to predict some long-range
395 contacts.

396 **Table 11.** The long- and medium-range contact prediction accuracy of our method, MetaPSICOV and
397 CCMpred on the CAMEO target 5djeB.

	Long range accuracy				Medium range accuracy			
	L	L/2	L/5	L/10	L	L/2	L/5	L/10
Our method	0.300	0.357	0.500	0.714	0.186	0.229	0.357	0.357
metaPSICOV	0.193	0.200	0.286	0.286	0.100	0.143	0.214	0.286
CCMpred	0.079	0.114	0.107	0.214	0.036	0.029	0.071	0.143

398

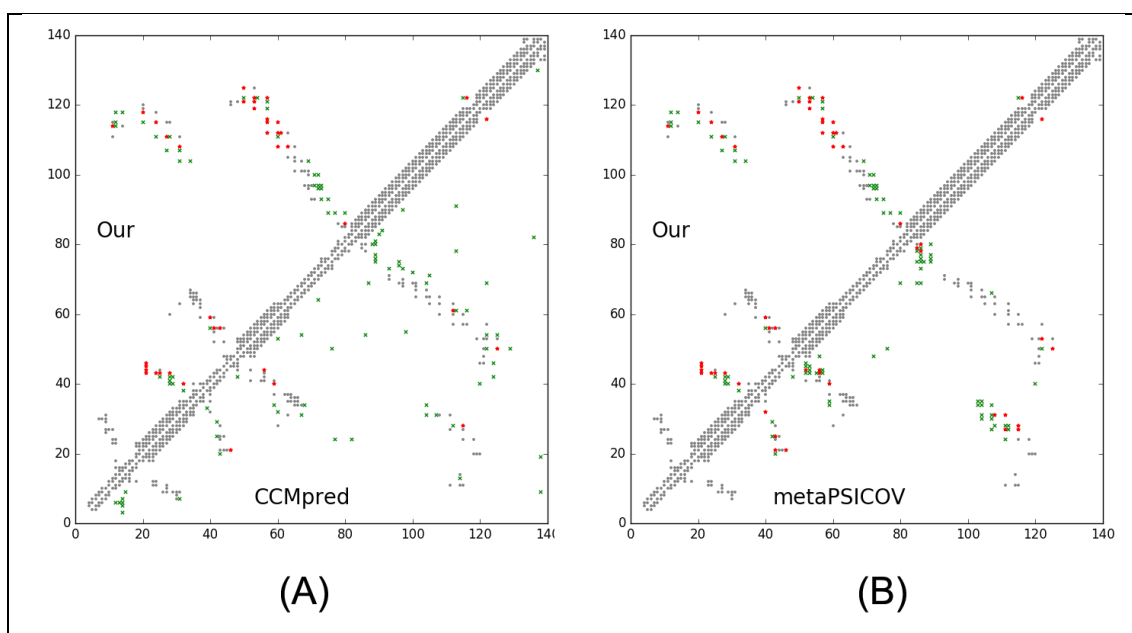
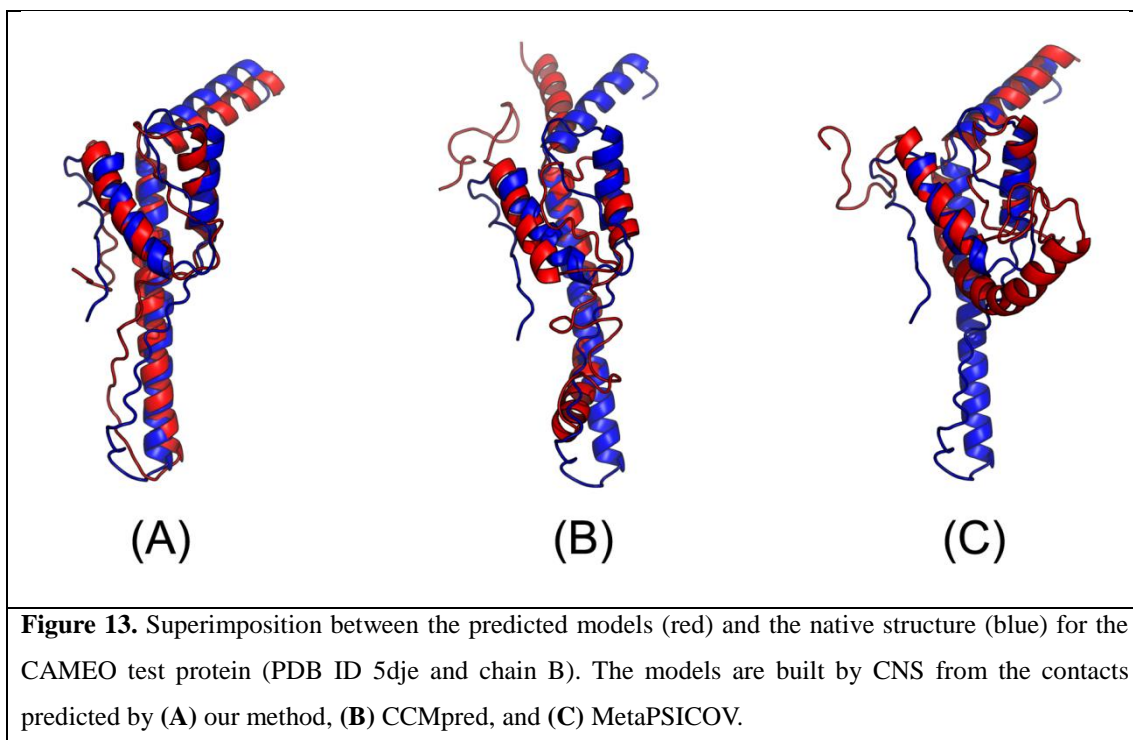


Figure 12. Overlap between top L/2 predicted contacts (in red and green) and the native (in grey). Red (green) dots indicate correct (incorrect) prediction. The left picture shows the comparison between our prediction (in upper-left triangle) and CCMpred (in lower-right triangle) and the right picture shows the comparison between our prediction (in upper-left triangle) and MetaPSICOV (in lower-right triangle).

399

400 The first 3D model submitted by our contact server has TMscore 0.65, while the best of our 5 models
401 has TMscore 0.65 and RMSD 5.6Å. By contrast, the best of top 5 models built by CNS from

402 CCMpred- and MetaPSICOV-predicted contacts have TMscore 0.404 and 0.427, respectively. Fig.
403 13(A) shows that all the four alpha helices of our predicted model (in red) matches well with the native
404 structure (blue), while the models from CCMpred (Fig. 13(B)) and MetaPSICOV (Fig. 13(C)) fail to
405 predict the 3rd long helix correctly. To examine the superimposition of our model with its native
406 structure from various angles, please see <http://raptorx.uchicago.edu/DeepAlign/26652330/>. Further, all
407 other CAMEO registered servers, including the top-notch servers such as HHpred, RaptorX,
408 SPARKS-X, and RBO Aleph (template-based and ab initio folding) only submitted models with
409 TMscore ≤ 0.35 , i.e., failed to predict a correct fold (Fig. 14).



410

411 This test protein represents a novel fold. Searching through PDB70 created right before September 24,
412 2016 by our in-house structural homolog search tool DeepSearch cannot identify structurally similar
413 proteins for this test protein. The most structurally similar proteins are 1u71A and 4x5uA, which have
414 TMscore 0.439 and 0.442 with the test protein, respectively. This is consistent with the fact that none of
415 the template-based CAMEO-participating servers predicted a good model for this test protein. By
416 contrast, our contact-assisted model has TMscore 0.65, much better than all the template-based models.

Server Name	Predictions	Resp. time (hh:mm:ss)	From	To	Cov (%)	IDDT	IDDT Ca	Avg. IDDT- BS	Avg. IDDT- BS details	QScore	QScore details	CAD- Score	GDT_HA	RMSD	GDC	Model Conf.	MaxSub	TMScore
Server 60	Model 1	19:20:14	1	140	100	54.43	68.22	-	-	-	-	0.60	36.03	5.81	45.19	0.50	0.51	0.65
RaptorX	Model 1	14:50:24	1	140	100	33.59	42.23	-	-	-	-	0.53	18.93	18.88	19.98	0.71	0.22	0.34
RBO Aleph	Model 1	53:34:20	1	140	100	40.65	50.35	-	-	-	-	0.56	18.57	14.98	18.37	0.50	0.19	0.31
Server 45	Model 1	36:00:52	1	140	100	35.96	44.10	-	-	-	-	0.53	19.12	20.97	20.16	0.67	0.21	0.31
SPARKS-X	Model 1	01:34:53	1	140	100	34.24	43.59	-	-	-	-	0.51	16.54	24.40	15.18	0.53	0.19	0.27
IntiFOLD3-TS	Model 1	23:58:21	1	140	100	33.49	41.34	-	-	-	-	0.49	16.91	25.85	14.94	0.75	0.18	0.26
Princeton_TEMPLATE	Model 1	05:43:56	1	140	100	35.77	44.78	-	-	-	-	0.53	20.22	23.15	15.79	0.50	0.21	0.26
Server 56	Model 1	22:29:49	1	140	100	34.96	43.55	-	-	-	-	0.48	15.44	23.61	14.73	0.96	0.17	0.26
Server 58	Model 1	22:29:22	1	140	100	34.96	43.55	-	-	-	-	0.48	15.44	23.61	14.73	0.96	0.17	0.26
Server 57	Model 1	22:29:51	1	140	100	34.09	42.06	-	-	-	-	0.50	16.54	26.14	14.42	0.82	0.18	0.25
Server 7	Model 1	18:14:55	81	140	42	15.51	20.19	-	-	-	-	0.25	16.18	14.71	15.77	0.58	0.19	0.22
HHpredB	Model 1	00:08:59	1	140	100	32.19	41.28	-	-	-	-	0.53	14.71	36.79	12.95	0.61	0.15	0.21
Server 55	Model 1	00:35:17	1	140	100	30.19	37.98	-	-	-	-	0.53	16.36	35.62	14.87	0.66	0.17	0.21
SWISS-MODEL	Model 1	00:00:14	86	127	30	9.27	12.47	-	-	-	-	0.17	16.18	11.45	14.77	0.92	0.17	0.19
Server 46	Model 1	00:03:45	86	127	30	9.27	12.47	-	-	-	-	0.17	16.18	11.45	14.77	0.92	0.17	0.19

417

418 **Figure 14.** The list of CAMEO-participating servers (only 15 of 20 are displayed) and their model
419 scores. The rightmost column displays the TMScore of submitted models. Server60 is our contact web
420 server.

421 **Study of CAMEO target 5f5pH (CAMEO ID: 2016-10-15_00000047_1, PDB ID: 5f5p)**

422 On October 15, 2016, our contact web server successfully folded a very hard and also
423 interesting CAMEO target (PDB ID: 5f5pH, CAMEO ID: 2016-10-15_00000047_1). This
424 target is an alpha protein of 217 residues with four helices. Table 12 shows that our server
425 produced a much better long-range contact prediction than CCMpred and MetaPSICOV.
426 Specifically, our contact prediction has L/5 and L/10 long-range accuracy 76.7% and 95.2%,
427 respectively, while MetaPSICOV has L/5 and L/10 accuracy less than 40%. CCMpred has
428 very low accuracy since this target has only ~65 non-redundant sequence homologs, i.e., its
429 Meff=65. The three methods have low L/k (k=1, 2) medium-range accuracy because there are fewer
430 than L/k native medium-range contacts while we use L/k as the denominator in calculating accuracy.
431 As shown in Fig. 15, CCMpred predicts too many false positives while MetaPSICOV predicts
432 very few correct long-range contacts.

433 **Table 12.** The long- and medium-range contact prediction accuracy of our method, MetaPSICOV and
434 CCMpred on the CAMEO target 5f5pH.

	Long-range accuracy				Medium-range accuracy			
	L	L/2	L/5	L/10	L	L/2	L/5	L/10
Our server	0.382	0.602	0.767	0.952	0.041	0.083	0.209	0.381
metaPSICOV	0.161	0.250	0.326	0.476	0.041	0.083	0.163	0.190
CCMpred	0.032	0.037	0.047	0.048	0.009	0.019	0.023	0.032

435

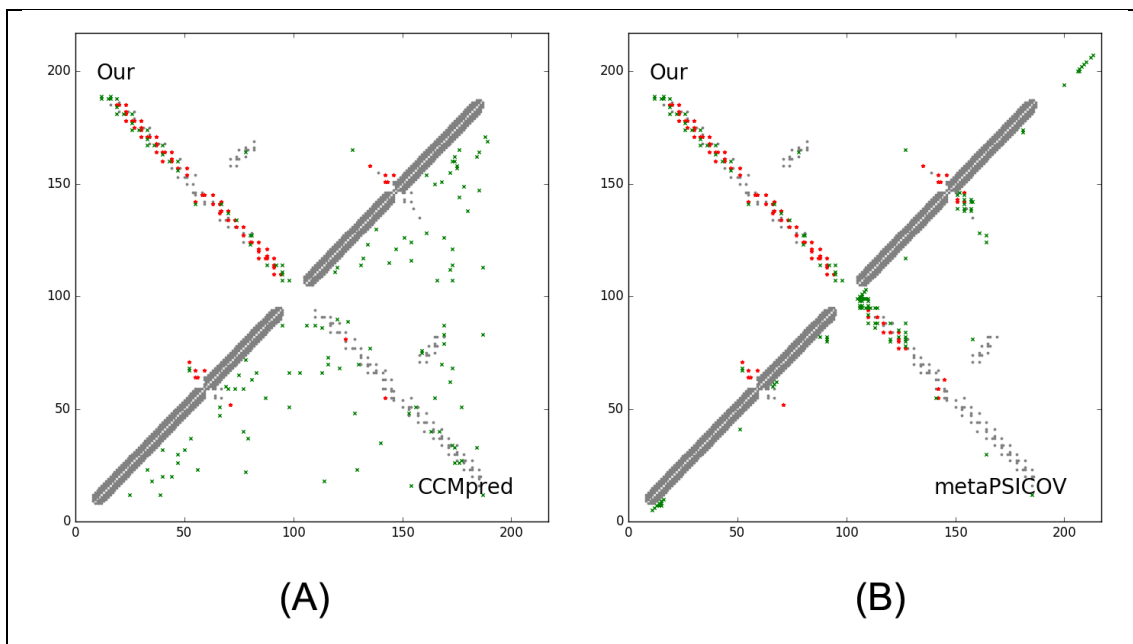
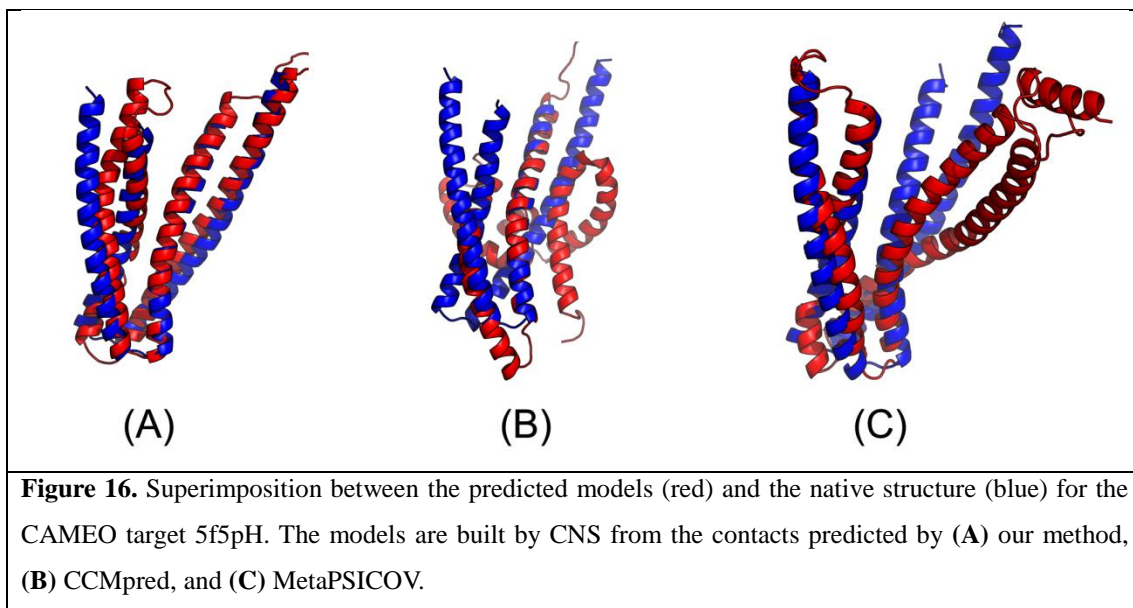


Figure 15. Overlap between top L/2 predicted contacts (in red and green) and the native (in grey). Red (green) dots indicate correct (incorrect) prediction. The left picture shows the comparison between our prediction (in upper-left triangle) and CCMpred (in lower-right triangle) and the right picture shows the comparison between our prediction (in upper-left triangle) and MetaPSICOV (in lower-right triangle).

436

437 Our submitted 3D model has TMscore 0.71 and RMSD 4.21Å. By contrast, the best of top 5 models
438 built by CNS from CCMpred- and MetaPSICOV-predicted contacts have TMscore 0.280 and 0.472,
439 respectively. Fig. 16(A) shows that our predicted model (in red) match well with the native structure
440 (blue), while the model from CCMpred (Fig. 16(B)) is completely wrong and the model from
441 MetaPSICOV (Fig. 16(C)) fails to place the 1st and 4th helices correctly. Please see
442 <http://raptorx.uchicago.edu/DeepAlign/14544627/> for the animated superimposition of our model with
443 its native structure. As shown in the ranking list (Fig. 17), all the other CAMEO-participating servers,
444 including Robetta, HHpred, RaptorX, SPARKS-X, and RBO Aleph (template-based and ab initio
445 folding) only submitted models with TMscore ≤ 0.48 and RMSD > 43.82Å. Our contact server is the
446 only one that predicted a correct fold for this target.



447

Server Name	Predictions	Resp. time (h:m:ss)	From	To	Cov. (%)	IDDT	IDDT C α	Avg IDDT-BS	Avg IDDT-BS details	QScore	QScore details	CAD- Score	GDT_HA	RMSD	GDC	Model Conf	MaxSub	TMscore
Server 60	Model 1	08:54:54	1	217	100	62.05	74.62	-	-	-	-	0.66	34.80	4.21	46.75	0.50	0.51	0.71
Server 55	Model 1	04:57:59	1	217	100	46.69	53.25	-	-	-	-	0.67	36.40	49.95	37.59	0.58	0.43	0.48
SWISS-MODEL	Model 1	00:00:55	10	189	82	46.62	53.11	-	-	-	-	0.66	36.55	50.09	37.53	0.60	0.43	0.48
Server 54	Model 1	04:33:36	10	189	82	46.62	53.11	-	-	-	-	0.66	36.55	50.09	37.53	0.60	0.43	0.48
Server 46	Model 1	03:38:25	10	189	82	46.43	53.18	-	-	-	-	0.66	36.99	50.09	37.55	0.58	0.44	0.48
Server 48	Model 1	00:03:54	10	189	82	46.43	53.18	-	-	-	-	0.66	36.99	50.09	37.55	0.58	0.44	0.48
Server 0	Model 1	00:31:28	10	189	82	45.68	53.07	-	-	-	-	0.65	36.70	50.10	37.30	0.65	0.43	0.47
Phyre2	Model 1	00:36:56	12	189	82	43.44	52.59	-	-	-	-	0.66	36.11	50.40	37.07	0.50	0.43	0.47
Server 19	Model 1	32:52:37	1	217	100	46.45	54.13	-	-	-	-	0.65	30.70	44.65	33.58	0.60	0.38	0.46
RaptorX	Model 1	11:27:06	1	217	100	43.71	52.40	-	-	-	-	0.62	27.34	50.41	31.75	0.60	0.36	0.44
Server 61	Model 1	00:08:19	10	189	82	45.47	52.90	-	-	-	-	0.66	31.43	49.27	31.78	0.56	0.35	0.43
Server 64	Model 1	00:22:11	10	189	82	45.47	52.90	-	-	-	-	0.66	31.43	49.27	31.78	0.56	0.35	0.43
Server 65	Model 1	00:10:21	10	189	82	45.47	52.90	-	-	-	-	0.66	31.43	49.27	31.78	0.56	0.35	0.43
Robetta	Model 1	22:40:39	1	217	100	45.01	52.84	-	-	-	-	0.64	30.41	43.82	31.63	0.89	0.35	0.42
M4T	Model 1	17:10:05	10	189	82	44.45	52.48	-	-	-	-	0.64	24.56	48.17	27.62	0.52	0.29	0.39

448

449 **Figure 17.** The list of CAMEO-participating servers (only 15 of 20 are displayed) and their model
 450 scores. The rightmost column displays the TMscore of submitted models. Server60 is our contact web
 451 server.

452 To make sure our best model is not simply copied from the database of solved structures, we search our
 453 best model against PDB70 created right before October 15, 2016 using our in-house structural homolog
 454 search tool DeepSearch, which yields two weakly similar proteins 2yfaA and 4k1pA. They have
 455 TMscore 0.536 and 0.511 with our best model, respectively. This implies that our model is not simply
 456 copied from a solved structure in PDB.

457 We ran BLAST on this target against PDB70 and surprisingly, found one protein 3thfA with E-value
 458 3E-16 and sequence identity 35%. In fact, 3thfA and 5f5pH are two SD2 proteins from Drosophila and
 459 Human(41), respectively. Although homologous, they adopt different conformations and
 460 oligomerizations. In particular, 3thfA is a dimer and each monomer adopts a fold consisting of three

461 segmented anti-parallel coiled-coil(42), whereas 5f5pH is a monomer that consists of two segmented
 462 antiparallel coiled-coils(41). Superimposing the Human SD2 monomer onto the Drosophila SD2 dimer
 463 shows that the former structure was located directly in between the two structurally identical halves of
 464 the latter structure (see Fig. 18(A)). That is, if our method predicts the contacts of 5f5pH by simply
 465 copying from 3thfA, it would produce a wrong 3D model. By contrast, all the other
 466 CAMEO-participating servers produced a wrong prediction for this target by using 3thfA as the
 467 template.

468 Since SD2 protein may have conformational change when docking with Rock SBD protein, we check
 469 if the Drosophila SD2 monomer would change to a similar fold as the Human SD2 monomer or not.
 470 According to(41), the Human SD2 adopts a similar fold no matter whether it docks with the Rock SBD
 471 or not. According to (42), although the Drosophila SD2 dimer may have conformational change in the
 472 presence of Rock, the change only occurs in the hinge regions, but not at the adjacent identical halves.
 473 That is, even conformational change happens, the Drosophila SD2 monomer would not resemble the
 474 Human SD2 monomer (Fig. 18(B)).

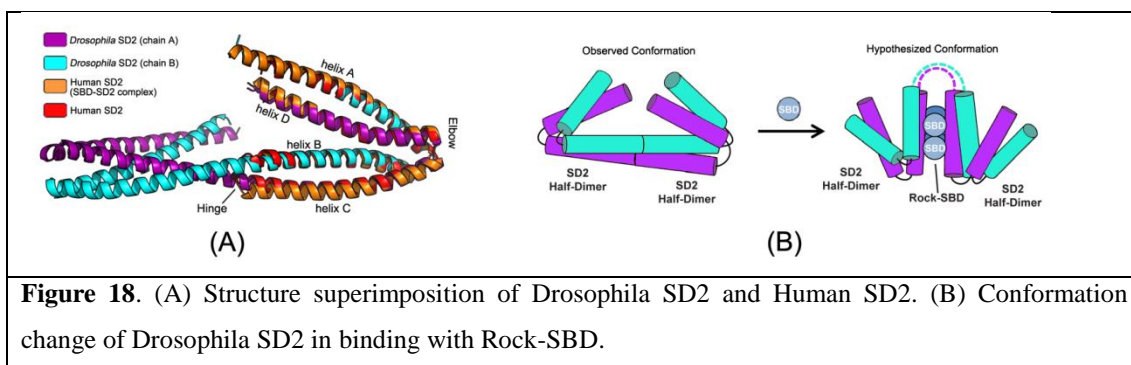


Figure 18. (A) Structure superimposition of Drosophila SD2 and Human SD2. (B) Conformation change of Drosophila SD2 in binding with Rock-SBD.

475 **Study of CAMEO target 5flgB (CAMEO ID: 2016-11-12_00000046_1, PDB ID: 5flgB)**

476 This target was released by CAMEO on November 12, 2016 and not included in the abovementioned
 477 41 CAMEO hard targets. This target is a unique α/β protein with 260 residues. Table 13 shows that our
 478 server produced a much better (long-range) contact prediction than CCMpred and MetaPSICOV. In
 479 particular, our predicted contact map has L, L/2, L/5 and L/10 long-range accuracy 71.1%, 86.1%, 96.1%
 480 and 100.0%, respectively, while CCMpred- and MetaPSICOV-predicted contacts have long-range
 481 accuracy less than 35% since there are only ~113 effective sequence homologs for this protein, i.e., its
 482 $M_{eff}=113$. Fig. 19 shows that both CCMpred and MetaPSICOV generated many false positive contact
 483 predictions and failed to predict long-range contacts.

484 **Table 13.** The long- and medium-range contact prediction accuracy of our method, MetaPSICOV and
 485 CCMpred on the CAMEO target 5flgB.

	Long-range accuracy				Medium-range accuracy			
	L	L/2	L/5	L/10	L	L/2	L/5	L/10
Our server	0.711	0.861	0.961	1.00	0.331	0.500	0.750	0.808
MetaPSICOV	0.208	0.262	0.269	0.288	0.242	0.285	0.442	0.615

CCMpred	0.165	0.184	0.308	0.346	0.150	0.215	0.346	0.385
---------	-------	-------	-------	-------	-------	-------	-------	-------

486

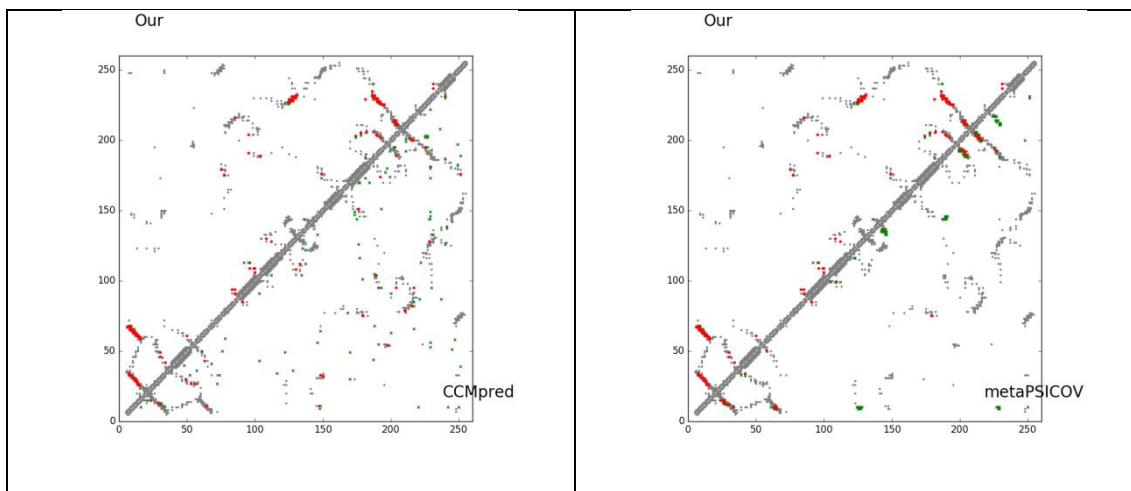


Figure 19. Overlap between predicted contacts (in red and green) and the native (in grey). Red (green) dots indicate correct (incorrect) prediction. Top L/2 predicted contacts by each method are shown. The left picture shows the comparison between our prediction (in upper-left triangle) and CCMpred (in lower-right triangle) and the right picture shows the comparison between our prediction (in upper-left triangle) and MetaPSICOV (in lower-right triangle).

487 The 3D model submitted by our contact server has TMscore 0.61 and RMSD 7.12Å. The best of top 5
 488 models built by CNS from CCMpred- and MetaPSICOV-predicted contacts have TMscore 0.240 and
 489 0.267, respectively. Fig. 20 shows that our method correctly modeled the overall fold, while CCMpred
 490 and MetaPSICOV failed. To examine the superimposition of our model with its native structure from
 491 various angles, please see <http://raptorx.uchicago.edu/DeepAlign/12043612/>. Furthermore, all the other
 492 CAMEO-participating servers, including the top-notch servers Robetta, HHpred, RaptorX, SPARKS-X,
 493 and RBO Aleph (template-based and ab initio folding), only submitted models with TMscore ≤ 0.25
 494 and RMSD $> 16.90\text{\AA}$ (Fig. 21). A 3D model with TMscore less than 0.25 does not have the correct fold
 495 while a model with TMscore ≥ 0.6 very likely has a correct fold. That is, our contact server predicted a
 496 correct fold for this target while the others failed to.

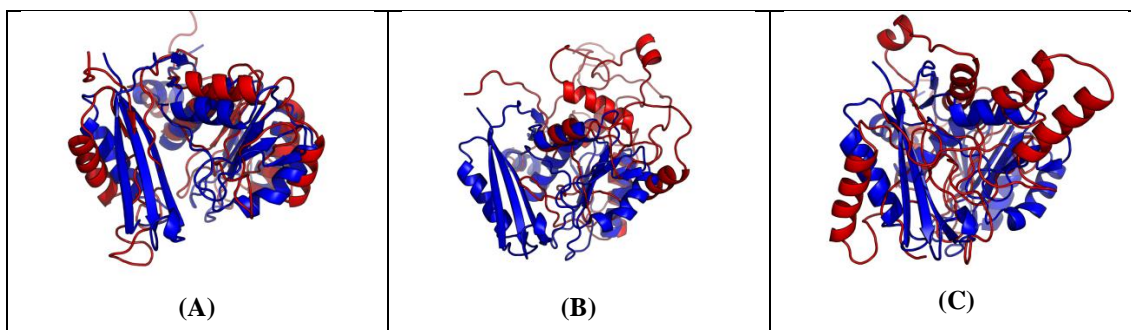


Figure 20. Superimposition between the predicted models (red) and the native structure (blue) for the CAMEO test protein 5flgB. The models are built by CNS from the contacts predicted by (A) our method, (B) CCMpred, and (C) MetaPSICOV.

497

498 This test protein has a novel fold. Searching through PDB70 created right before November 12, 2016
 499 by our in-house structural homolog search tool DeepSearch cannot identify any similar structures. The
 500 most structurally similar proteins returned by DeepSearch are 2fb5A and 5dwmA, which have TMScore
 501 0.367 and 0.355 with the native structure of this target, respectively. This is consistent with the fact that
 502 all the other CAMEO-participating servers failed to predict a correct fold for this target.

Server Name	Predictions	Resp. time (hh:mm:ss)	From	To	Cov (%)	IDDT	IDDT Co	Avg IDDT- BS	Avg. IDDT-BS details	QScore	QScore details	CAD- Score	GDT_HA	RMSD	GDC	Model Conf.	MaxSub	TMScore
Server 60	Model 1	23:01:01	1	260	100	40.26	48.52	49.57	PMLS:0.39(1.00) PML1:0.40(1.00) MG4:0.76(1.00) ANP2:0.33(1.00) ANPS:0.29(1.00) MGS:0.77(1.00)	-	-	0.46	21.53	7.12	32.36	0.50	0.30	0.61
Server 56	Model 1	25:20:28	1	260	100	23.25	28.04	42.32	PMLS:0.27(1.00) PML1:0.27(1.00) MG4:0.77(1.00) ANP2:0.24(1.00) ANPS:0.23(1.00) MGS:0.75(1.00)	-	-	0.37	7.14	22.73	8.39	0.75	0.07	0.24
Server 58	Model 1	25:19:10	1	260	100	23.25	28.04	42.32	PMLS:0.27(1.00) PML1:0.27(1.00) MG4:0.77(1.00) ANP2:0.24(1.00) ANPS:0.23(1.00) MGS:0.75(1.00)	-	-	0.37	7.14	22.73	8.39	0.75	0.07	0.24
Server 19	Model 1	49:15:36	1	260	100	22.45	26.66	44.73	PMLS:0.32(1.00) PML1:0.25(1.00) MG4:0.81(1.00) ANP2:0.26(1.00) ANPS:0.23(1.00) MGS:0.81(1.00)	-	-	0.39	9.23	24.62	10.31	0.79	0.11	0.23
Princeton_TEMPLATE	Model 1	01:24:35	1	260	100	20.05	24.37	39.67	PMLS:0.16(1.00) PML1:0.20(1.00) MG4:0.73(1.00) ANP2:0.29(1.00) ANPS:0.28(1.00) MGS:0.71(1.00)	-	-	0.33	7.24	26.50	7.35	0.57	0.07	0.22

503

504 **Figure 21.** The list of CAMEO-participating servers (only 5 of 26 are displayed) and their model
 505 scores. The rightmost column displays the model TMScore. Server60 is our contact web server.

506 Conclusion and Discussion

507 In this paper we have presented a new deep (supervised) learning method that can greatly improve
 508 protein contact prediction. Our method distinguishes itself from previous supervised learning methods
 509 in that we employ a concatenation of two deep residual neural networks to model sequence-contact
 510 relationship, one for modeling of sequential features (i.e., sequence profile, predicted secondary
 511 structure and solvent accessibility) and the other for modeling of pairwise features (e.g., coevolution
 512 information). Ultra-deep residual network is the latest breakthrough in computer vision and has
 513 demonstrated the best performance in the computer vision challenge tasks (similar to CASP) in 2015.
 514 Our method is also unique in that we predict all contacts of a protein simultaneously, which allows us
 515 to easily model high-order residue correlation. By contrast, existing supervised learning methods
 516 predict if two residues form a contact or not independent of the other residue pairs. Our (blind) test
 517 results show that our method dramatically improves contact prediction, exceeding currently the best
 518 methods (e.g., CCMpred, Evfold, PSICOV and MetaPSICOV) by a very large margin. Even without
 519 using any force fields and fragment assembly, ab initio folding using our predicted contacts as
 520 restraints can yield 3D structural models of correct fold for many test proteins. Further, our
 521 experimental results also show that our contact-assisted models are much better than template-based
 522 models built from the training proteins of our deep model. We expect that our contact prediction
 523 methods can help reveal much more biological insights for those protein families without solved
 524 structures and close structural homologs.

525 Our method outperforms ECA due to a couple of reasons. First, ECA predicts contacts using
526 information only in a single protein family, while our method learns sequence-structure relationship
527 from thousands of protein families. Second, ECA considers only pairwise residue correlation, while our
528 deep architecture can capture high-order residue correlation (or contact occurring patterns) very well.
529 Our method uses a subset of protein features used by MetaPSICOV, but performs much better than
530 MetaPSICOV mainly because we explicitly model contact patterns (or high-order correlation), which is
531 enabled by predicting contacts of a single protein simultaneously. MetaPSICOV employs a 2-stage
532 approach. The 1st stage predicts if there is a contact between a pair of residues independent of the other
533 residues. The 2nd stage considers the correlation between one residue pair and its neighboring pairs, but
534 not in a very good way. In particular, the prediction errors in the 1st stage of MetaPSICOV cannot be
535 corrected by the 2nd stage since two stages are trained separately. By contrast, we train all 2D
536 convolution layers simultaneously (each layer is equivalent to one stage) so that later stages can correct
537 prediction errors in early stages. In addition, a deep network can model much higher-order correlation
538 and thus, capture information in a much larger context.

539 Our deep model does not predict contact maps by simply recognizing them from PDB, as evidenced by
540 our experimental settings and results. First, we employ a strict criterion to remove redundancy so that
541 there are no training proteins with sequence identity >25% or BLAST E-value <0.1 with any test
542 proteins. Second, our contact-assisted models also have better quality than homology models, so it is
543 unlikely that our predicted contact maps are simply copied from the training proteins. Third, our deep
544 model trained by only non-membrane proteins works very well on membrane proteins. By contrast, the
545 homology models built from the training proteins for the membrane proteins have very low quality.
546 Their average TMscore is no more than 0.17, which is the expected TMscore of any two
547 randomly-chosen proteins. Finally, the blind CAMEO test indicates that our method successfully
548 folded several targets with a new fold (e.g., 5f5pH).

549 We have studied the impact of different input features. First of all, the co-evolution strength produced
550 by CCMpred is the most important input features. Without it, the top L/10 long-range prediction
551 accuracy may drop by 0.15 for soluble proteins and more for membrane proteins. The larger
552 performance degradation for membrane proteins is mainly because information learned from sequential
553 features of soluble proteins is not useful for membrane proteins. The depth of our deep model is equally
554 important, as evidenced by the fact that our deep method has much better accuracy than MetaPSICOV
555 although we use a subset of protein features used by MetaPSICOV. Our test shows that a deep model
556 with 9 and 30 layers have top L/10 accuracy ~0.1 and ~0.03 worse than a 60-layer model, respectively.
557 This suggests that it is very important to model contact occurring patterns (i.e., high-order residue
558 correlation) by a deep architecture. The pairwise contact potential and mutual information may impact
559 the accuracy by 0.02-0.03. The secondary structure and solvent accessibility may impact the accuracy
560 by 0.01-0.02.

561 An interesting finding is that although our training set contains only ~100 membrane proteins, our
562 model works well for membrane proteins, much better than CCMpred and MetaPSICOV. Even without

563 using any membrane proteins in our training set, our deep models have almost the same accuracy on
564 membrane proteins as those trained with membrane proteins. This implies that the sequence-structure
565 relationship learned by our model from non-membrane proteins can generalize well to membrane
566 protein contact prediction. We are going to study if we can further improve contact prediction accuracy
567 of membrane proteins by including many more membrane proteins in the training set.

568 We may further improve contact prediction accuracy by enlarging the training set. First, the latest
569 PDB25 has more than 10,000 proteins, which can provide many more training proteins than what we
570 are using now. Second, when removing redundancy between training and test proteins, we may relax
571 the BLAST E-value cutoff to 0.001 or simply drop it. This will improve the top L/k (k=1,2,5,10)
572 contact prediction accuracy by 1-3% and accordingly the quality of the resultant 3D models by
573 0.01-0.02 in terms of TMscore. **We may also improve the 3D model quality by combining our predicted
574 contacts with energy function and fragment assembly. For example, we may feed our predicted contacts
575 to Rosetta to build 3D models. Compared to CNS, Rosetta makes use of energy function and more
576 local structural restraints through fragment assembly and thus, shall result in much better 3D models.
577 Finally, instead of predicting contacts, our deep learning model actually can predict inter-residue
578 distance distribution (i.e., distance matrix), which provides finer-grained information than contact maps
579 and thus, shall benefit 3D structure modeling more than predicted contacts.**

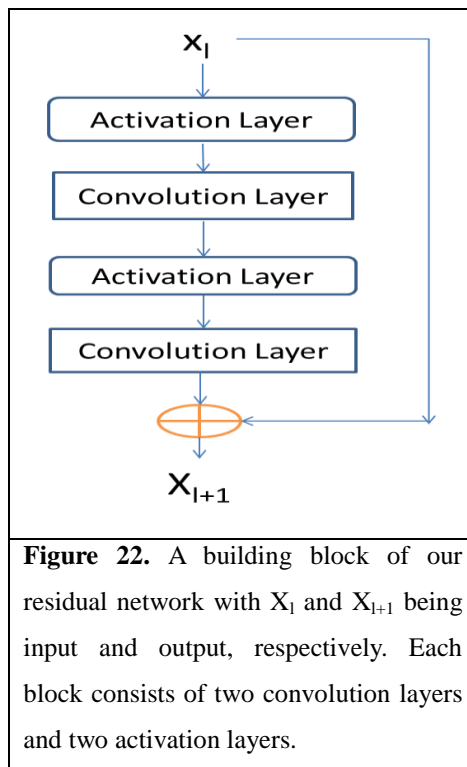
580 Our model achieves pretty good performance when using around 60-70 convolutional layers. A natural
581 question to ask is can we further improve prediction accuracy by using many more convolutional layers?
582 In computer vision, it has been shown that a 1001-layer residual neural network can yield better
583 accuracy for image-level classification than a 100-layer network (but no result on pixel-level labeling is
584 reported). Currently we cannot apply more than 100 layers to our model due to insufficient memory of
585 a GPU card (12G). We plan to overcome the memory limitation by extending our training algorithm to
586 run on multiple GPU cards. Then we will train a model with hundreds of layers to see if we can further
587 improve prediction accuracy or not.

588 Method

589 Deep learning model details

590 **Residual network blocks.** Our network consists of two
591 residual neural networks, each in turn consisting of some
592 residual blocks concatenated together. Fig. 22 shows an
593 example of a residual block consisting of 2 convolution
594 layers and 2 activation layers. In this figure, X_i and X_{i+1}
595 are the input and output of the block, respectively. The
596 activation layer conducts a simple nonlinear
597 transformation of its input without using any parameters.
598 Here we use the ReLU activation function (30) for such a
599 transformation. Let $f(X_i)$ denote the result of X_i going
600 through the two activation layers and the two convolution
601 layers. Then, X_{i+1} is equal to $X_i + f(X_i)$. That is, X_{i+1} is a
602 combination of X_i and its nonlinear transformation. Since
603 $f(X_i)$ is equal to the difference between X_{i+1} and X_i , f is
604 called residual function and this network called residual
605 network. In the first residual network, X_i and X_{i+1}
606 represent sequential features and have dimension $L \times n_i$ and
607 $L \times n_{i+1}$, respectively, where L is protein sequence length

608 and n_i (n_{i+1}) can be interpreted as the number of features or hidden neurons at each position (i.e.,
609 residue). In the 2nd residual network, X_i and X_{i+1} represent pairwise features and have dimension $L \times L$
610 $\times n_i$ and $L \times L \times n_{i+1}$, respectively, where n_i (n_{i+1}) can be interpreted as the number of features or hidden
611 neurons at one position (i.e., residue pair). Typically, we enforce $n_i \leq n_{i+1}$ since one position at a higher
612 level is supposed to carry more information. When $n_i < n_{i+1}$, in calculating $X_i + f(X_i)$ we shall pad zeros
613 to X_i so that it has the same dimension as X_{i+1} . To speed up training, we also add a batch normalization
614 layer (43) before each activation layer, which normalizes its input to have mean 0 and standard
615 deviation 1. The filter size (i.e., window size) used by a 1D convolution layer is 17 while that used by a
616 2D convolution layer is 3×3 or 5×5 . By stacking many residual blocks together, even if at each
617 convolution layer we use a small window size, our network can model very long-range
618 interdependency between input features and contacts as well as the long-range interdependency
619 between two different residue pairs. We fix the depth (i.e., the number of convolution layers) of the 1D
620 residual network to 6, but vary the depth of the 2D residual network. Our experimental results show
621 that with ~ 60 hidden neurons at each position and ~ 60 convolution layers for the 2nd residual network,
622 our model can yield pretty good performance. Note that it has been shown that for image classification
623 a convolutional neural network with a smaller window size but many more layers usually outperforms
624 a network with a larger window size but fewer layers. Further, a 2D convolutional neural network with
625 a smaller window size also has a smaller number of parameters than a network with a larger window



626 size. See <https://github.com/KaimingHe/deep-residual-networks> for some existing implementations of
627 2D residual neural network. However, they assume an input of fixed dimension, while our network
628 needs to take variable-length proteins as input.

629 Our deep learning method for contact prediction is unique in at least two aspects. First, our model
630 employs two multi-layer residual neural networks, which have not been applied to contact prediction
631 before. Residual neural networks can pass both linear and nonlinear information from end to end (i.e.,
632 from the initial input to the final output). Second, we do contact prediction on the whole contact map
633 by treating it as an individual image. In contrast, previous supervised learning methods separate the
634 prediction of one residue pair from the others. By predicting contacts of a protein simultaneously, we
635 can easily model long-range contact correlation and high-order residue correlation and long-range
636 correlation between a contact and input features.

637 **Convolutional operation.** Existing deep learning development toolkits such as Theano
638 (<http://deeplearning.net/software/theano/>) and Tensorflow (<https://www.tensorflow.org/>) have provided
639 an API (application programming interface) for convolutional operation so that we do not need to
640 implement it by ourselves. See <http://deeplearning.net/tutorial/lenet.html> and
641 <https://www.nervanasys.com/convolutional-neural-networks/> for a good tutorial of convolutional
642 network. Please also see (44) for a detailed account of 1D convolutional network with application to
643 protein sequence labeling. Roughly, a 1D convolution operation is de facto matrix-vector multiplication
644 and 2D convolution can be interpreted similarly. Let X and Y (with dimensions $L \times m$ and $L \times n$,
645 respectively) be the input and output of a 1D convolutional layer, respectively. Let the window size be
646 $2w+1$ and $s=(2w+1)m$. The convolutional operator that transforms X to Y can be represented as a 2D
647 matrix with dimension $n \times s$, denoted as C . C is protein length-independent and each convolutional layer
648 may have a different C . Let X_i be a submatrix of X centered at residue i ($1 \leq i \leq L$) with dimension
649 $(2w+1) \times m$, and Y_i be the i -th row of Y . We may calculate Y_i by first flattening X_i to a vector of length s
650 and then multiplying C and the flattened X_i .

651 **Conversion of sequential features to pairwise features.** We convert the output of the first module of
652 our model (i.e., the 1-d residual neural network) to a 2D representation using an operation similar to
653 outer product. Simply speaking, let $v = \{v_1, v_2, \dots, v_i, \dots, v_L\}$ be the final output of the first module
654 where L is protein sequence length and v_i is a feature vector storing the output information for residue i .
655 For a pair of residues i and j , we concatenate v_i , $v_{(i+j)/2}$ and v_j to a single vector and use it as one input
656 feature of this residue pair. The input features for this pair also include mutual information, the EC
657 information calculated by CCMpred and pairwise contact potential (45, 46).

658 **Loss function.** We use maximum-likelihood method to train model parameters. That is, we maximize
659 the occurring probability of the native contacts (and non-contacts) of the training proteins. Therefore,
660 the loss function is defined as the negative log-likelihood averaged over all the residue pairs of the
661 training proteins. Since the ratio of contacts among all the residue pairs is very small, to make the
662 training algorithm converge fast, we assign a larger weight to the residue pairs forming a contact. The
663 weight is assigned such that the total weight assigned to contacts is approximately 1/8 of the number of

664 non-contacts in the training set.

665 **Regularization and optimization.** To prevent overfitting, we employ L_2 -norm regularization to reduce
666 the parameter space. That is, we want to find a set of parameters with a small L_2 norm to minimize the
667 loss function, so the final objective function to be minimized is the sum of loss function and the L_2
668 norm of the model parameters (multiplied by a regularization factor). We use a stochastic gradient
669 descent algorithm to minimize the objective function. It takes 20-30 epochs (each epoch scans through
670 all the training proteins exactly once) to obtain a very good solution. The whole algorithm is
671 implemented by Theano (47) and mainly runs on GPU.

672 **Training and dealing with proteins of different lengths.** Our network can take as input
673 variable-length proteins. We train our deep network in a minibatch mode, which is routinely used in
674 deep learning. That is, at each iteration of our training algorithm, we use a minibatch of proteins to
675 calculate gradient and update the model parameters. A minibatch may have one or several proteins. We
676 sort all training proteins by length and group proteins of similar lengths into minibatches. Considering
677 that most proteins have length up to 600 residues, proteins in a minibatch often have the same length.
678 In the case that they do not, we add zero padding to shorter proteins. Our convolutional operation is
679 protein-length independent, so two different minibatches are allowed to have different protein lengths.
680 We have tested minibatches with only a single protein or with several proteins. Both work well.
681 However, it is much easier to implement minibatches with only a single protein.

682 Since our network can take as input variable-length lengths, we do not need to cut a long protein into
683 segments in predicting contact maps. Instead we predict contacts in the whole chain simultaneously.
684 There is no need to use zero padding when only a single protein is predicted in a batch. Zero padding is
685 needed only when several proteins of different lengths are predicted in a batch.

686 **Training and test data**

687 Our test data includes the 150 Pfam families (5), 105 CASP11 test proteins, 76 hard CAMEO test
688 proteins released in 2015 (Supplementary Table 1) and 398 membrane proteins (Supplementary Table
689 2). All test membrane proteins have length no more than 400 residues and any two membrane proteins
690 share less than 40% sequence identity. For the CASP test proteins, we use the official domain
691 definitions, but we do not parse a CAMEO or membrane protein into domains.

692 Our training set is a subset of PDB25 created in February 2015, in which any two proteins share less
693 than 25% sequence identity. We exclude a protein from the training set if it satisfies one of the
694 following conditions: (i) sequence length smaller than 26 or larger than 700, (ii) resolution worse than
695 2.5Å, (iii) has domains made up of multiple protein chains, (iv) no DSSP information, and (v) there is
696 inconsistency between its PDB, DSSP and ASTRAL sequences (48). To remove redundancy with the
697 test sets, we exclude any training proteins sharing >25% sequence identity or having BLAST E-value
698 <0.1 with any test proteins. In total there are 6767 proteins in our training set, from which we have
699 trained 7 different models. For each model, we randomly sampled ~6000 proteins from the training set
700 to train the model and used the remaining proteins to validate the model and determine the

701 hyper-parameters (i.e., regularization factor). The final model is the average of these 7 models.

702 Protein features

703 We use similar but fewer protein features as MetaPSICOV. In particular, the input features include
704 protein sequence profile (i.e., position-specific scoring matrix), predicted 3-state secondary structure
705 and 3-state solvent accessibility, direct co-evolutionary information generated by CCMpred, mutual
706 information and pairwise potential (45, 46). To derive these features, we need to generate MSA
707 (multiple sequence alignment). For a training protein, we run PSI-BLAST (with E-value 0.001 and 3
708 iterations) to search the NR (non-redundant) protein sequence database dated in October 2012 to find
709 its sequence homologs, and then build its MSA and sequence profile and predict other features (i.e.,
710 secondary structure and solvent accessibility). **Sequence profile is represented as a 2D matrix with
711 dimension $L \times 20$ where L is the protein length. Predicted secondary structure is represented as a 2D
712 matrix with dimension $L \times 3$ (each entry is a predicted score or probability), so is the predicted solvent
713 accessibility. Concatenating them together, we have a 2D matrix with dimension $L \times 26$, which is the
714 input of our 1D residual network.**

715 For a test protein, we generate four different MSAs by running HHblits (38) with 3 iterations and
716 E-value set to 0.001 and 1, respectively, to search through the uniprot20 HMM library released in
717 November 2015 and February 2016. From each individual MSA, we derive one sequence profile and
718 employ our in-house tool RaptorX-Property (49) to predict the secondary structure and solvent
719 accessibility accordingly. That is, for each test protein we generate 4 sets of input features and
720 accordingly 4 different contact predictions. Then we average these 4 predictions to obtain the final
721 contact prediction. This averaged contact prediction is about 1-2% better than that predicted from a
722 single set of features (detailed data not shown). Although currently there are quite a few packages that
723 can generate direct evolutionary coupling information, we only employ CCMpred to do so because it
724 runs fast on GPU (4).

725 Programs to compare and evaluation metrics

726 We compare our method with PSICOV (5), Evfold (6), CCMpred (4), plmDCA, Gremlin, and
727 MetaPSICOV (9). The first 5 methods conduct pure DCA while MetaPSICOV employs supervised
728 learning. MetaPSICOV (9) performed the best in CASP11 (31). CCMpred, plmDCA, Gremlin perform
729 similarly, but better than PSICOV and Evfold. All the programs are run with parameters set according
730 to their respective papers. We evaluate the accuracy of the top L/k ($k=10, 5, 2, 1$) predicted contacts
731 where L is protein sequence length. The prediction accuracy is defined as the percentage of native
732 contacts among the top L/k predicted contacts. We also divide contacts into three groups according to
733 the sequence distance of two residues in a contact. That is, a contact is short-, medium- and long-range
734 when its sequence distance falls into $[6, 11]$, $[12, 23]$, and ≥ 24 , respectively.

735 Calculation of Meff

736 Meff measures the amount of homologous information in an MSA (multiple sequence alignment). It

737 can be interpreted as the number of non-redundant sequence homologs in an MSA when 70% sequence
738 identity is used as cutoff. To calculate M_{eff} , we first calculate the sequence identity between any two
739 proteins in the MSA. Let a binary variable S_{ij} denote the similarity between two protein sequences i and
740 j . S_{ij} is equal to 1 if and only if the sequence identity between i and j is at least 70%. For a protein i , we
741 calculate the sum of S_{ij} over all the proteins (including itself) in the MSA and denote it as S_i . Finally,
742 we calculate M_{eff} as the sum of $1/S_i$ over all the protein sequences in this MSA.

743 **3D model construction by contact-assisted folding**

744 We use a similar approach as described in (11) to build the 3D models of a test protein by feeding
745 predicted contacts and secondary structure to the Crystallography & NMR System (CNS) suite (32).
746 We predict secondary structure using our in-house tool RaptorX-Property (49) and then convert it to
747 distance, angle and h-bond restraints using a script in the Confold package (11). For each test protein,
748 we choose top 2L predicted contacts (L is sequence length) no matter whether they are short-, medium-
749 or long-range and then convert them to distance restraints. That is, a pair of residues predicted to form a
750 contact is assumed to have distance between 3.5 Å and 8.0 Å. In current implementation, we do not use
751 any force fields to help with folding. We generate twenty 3D structure models using CNS and select top
752 5 models by the NOE score yielded by CNS(32). The NOE score mainly reflects the degree of violation
753 of the model against the input constraints (i.e., predicted secondary structure and contacts). The lower
754 the NOE score, the more likely the model has a higher quality. When CCMpred- and
755 MetaPSICOV-predicted contacts are used to build 3D models, we also use the secondary structure
756 predicted by RaptorX-Property to warrant a fair comparison.

757 **Template-based modeling (TBM) of the test proteins**

758 To generate template-based models (TBMs) for a test protein, we first run HHblits (with the
759 UniProt20_2016 library) to generate an HMM file for the test protein, then run HHsearch with this
760 HMM file to search for the best templates among the 6767 training proteins of our deep learning model,
761 and finally run MODELLER to build a TBM from each of the top 5 templates.

762 **Author contributions**

763 J.X. conceived the project, developed the algorithm and wrote the paper. S.W. did data preparation and
764 analysis and helped with algorithm development and paper writing. S.S. helped with algorithm
765 development and data analysis. R.Z. helped with data analysis. Z.L. helped with algorithm
766 development.

767 **Acknowledgements**

768 This work is supported by National Institutes of Health grant R01GM089753 to J.X. and National
769 Science Foundation grant DBI-1564955 to J.X. The authors are also grateful to the support of Nvidia
770 Inc. and the computational resources provided by XSEDE.

771 **References**

- 772 1. Kim DE, DiMaio F, Yu - Rwei Wang R, Song Y, Baker D. One contact for every twelve residues
773 allows robust and accurate topology - level protein structure modeling. *Proteins: Structure, Function,
774 and Bioinformatics*. 2014;82(S2):208-18.
- 775 2. de Juan D, Pazos F, Valencia A. Emerging methods in protein co-evolution. *Nature Reviews
776 Genetics*. 2013;14(4):249-61.
- 777 3. Weigt M, White RA, Szurmant H, Hoch JA, Hwa T. Identification of direct residue contacts in
778 protein-protein interaction by message passing. *P Natl Acad Sci USA*. 2009 Jan 6;106(1):67-72.
- 779 4. Seemayer S, Gruber M, Söding J. CCMpred—fast and precise prediction of protein residue–
780 residue contacts from correlated mutations. *Bioinformatics*. 2014;30(21):3128-30.
- 781 5. Jones DT, Buchan DW, Cozzetto D, Pontil M. PSICOV: precise structural contact prediction using
782 sparse inverse covariance estimation on large multiple sequence alignments. *Bioinformatics*.
783 2012;28(2):184-90.
- 784 6. Marks DS, Colwell LJ, Sheridan R, Hopf TA, Pagnani A, Zecchina R, et al. Protein 3D structure
785 computed from evolutionary sequence variation. *PloS one*. 2011;6(12):e28766.
- 786 7. Ekeberg M, Hartonen T, Aurell E. Fast pseudolikelihood maximization for direct-coupling
787 analysis of protein structure from many homologous amino-acid sequences. *J Comput Phys*. 2014 Nov
788 1;276:341-56.
- 789 8. Kamisetty H, Ovchinnikov S, Baker D. Assessing the utility of coevolution-based residue–residue
790 contact predictions in a sequence-and structure-rich era. *Proceedings of the National Academy of
791 Sciences*. 2013;110(39):15674-9.
- 792 9. Jones DT, Singh T, Kosciolk T, Tetchner S. MetaPSICOV: combining coevolution methods for
793 accurate prediction of contacts and long range hydrogen bonding in proteins. *Bioinformatics*.
794 2015;31(7):999-1006.
- 795 10. Ma J, Wang S, Wang Z, Xu J. Protein contact prediction by integrating joint evolutionary coupling
796 analysis and supervised learning. *Bioinformatics*. 2015:btv472.
- 797 11. Adhikari B, Bhattacharya D, Cao R, Cheng J. CONFOLD: residue - residue contact - guided ab
798 initio protein folding. *Proteins: Structure, Function, and Bioinformatics*. 2015;83(8):1436-49.
- 799 12. Wang S, Li W, Zhang R, Liu S, Xu J. CoinFold: a web server for protein contact prediction and
800 contact-assisted protein folding. *Nucleic acids research*. 2016:gkw307.
- 801 13. Di Lena P, Nagata K, Baldi P. Deep architectures for protein contact map prediction.
802 *Bioinformatics*. 2012;28(19):2449-57.
- 803 14. Ekeberg M, Lövkvist C, Lan Y, Weigt M, Aurell E. Improved contact prediction in proteins: using
804 pseudolikelihoods to infer Potts models. *Phys Rev E*. 2013;87(1):012707.
- 805 15. Göbel U, Sander C, Schneider R, Valencia A. Correlated mutations and residue contacts in
806 proteins. *Proteins: Structure, Function, and Bioinformatics*. 1994;18(4):309-17.
- 807 16. Morcos F, Pagnani A, Lunt B, Bertolino A, Marks DS, Sander C, et al. Direct-coupling analysis of
808 residue coevolution captures native contacts across many protein families. *Proceedings of the National*

- 809 Academy of Sciences. 2011;108(49):E1293-E301.
- 810 17. Skwark MJ, Raimondi D, Michel M, Elofsson A. Improved contact predictions using the
811 recognition of protein like contact patterns. *PLoS Comput Biol.* 2014;10(11):e1003889.
- 812 18. Wu S, Zhang Y. A comprehensive assessment of sequence-based and template-based methods for
813 protein contact prediction. *Bioinformatics.* 2008;24(7):924-31.
- 814 19. Wang Z, Xu J. Predicting protein contact map using evolutionary and physical constraints by
815 integer programming. *Bioinformatics.* 2013;29(13):i266-i73.
- 816 20. He K, Zhang X, Ren S, Sun J. Deep residual learning for image recognition. *arXiv preprint*
817 *arXiv:151203385.* 2015.
- 818 21. Krizhevsky A, Hinton G. Convolutional deep belief networks on cifar-10. Unpublished
819 manuscript. 2010;40.
- 820 22. Srivastava RK, Greff K, Schmidhuber J, editors. Training very deep networks. *Advances in neural*
821 *information processing systems;* 2015.
- 822 23. Hinton G, Deng L, Yu D, Dahl GE, Mohamed A-r, Jaitly N, et al. Deep neural networks for
823 acoustic modeling in speech recognition: The shared views of four research groups. *IEEE Signal*
824 *Processing Magazine.* 2012;29(6):82-97.
- 825 24. LeCun Y, Bengio Y, Hinton G. Deep learning. *Nature.* 2015;521(7553):436-44.
- 826 25. Szegedy C, Liu W, Jia Y, Sermanet P, Reed S, Anguelov D, et al., editors. Going deeper with
827 convolutions. *Proceedings of the IEEE Conference on Computer Vision and Pattern Recognition;* 2015.
- 828 26. Moult J, Fidelis K, Kryshtafovych A, Schwede T, Tramontano A. Critical assessment of methods
829 of protein structure prediction (CASP)—round x. *Proteins: Structure, Function, and Bioinformatics.*
830 2014;82(S2):1-6.
- 831 27. Moult J, Fidelis K, Kryshtafovych A, Schwede T, Tramontano A. Critical assessment of methods
832 of protein structure prediction: Progress and new directions in round XI. *Proteins: Structure, Function,*
833 *and Bioinformatics.* 2016.
- 834 28. Haas J, Roth S, Arnold K, Kiefer F, Schmidt T, Bordoli L, et al. The Protein Model Portal—a
835 comprehensive resource for protein structure and model information. *Database.* 2013;2013:bat031.
- 836 29. Pinheiro PH, Collobert R, editors. Recurrent Convolutional Neural Networks for Scene Labeling.
837 *ICML;* 2014.
- 838 30. Nair V, Hinton GE, editors. Rectified linear units improve restricted boltzmann machines.
839 *Proceedings of the 27th International Conference on Machine Learning (ICML-10);* 2010.
- 840 31. Monastyrskyy B, D'Andrea D, Fidelis K, Tramontano A, Kryshtafovych A. New encouraging
841 developments in contact prediction: Assessment of the CASP11 results. *Proteins: Structure, Function,*
842 *and Bioinformatics.* 2015.
- 843 32. Briinger AT, Adams PD, Clore GM, DeLano WL, Gros P, Grosse-Kunstleve RW, et al.
844 Crystallography & NMR system: A new software suite for macromolecular structure determination.
845 *Acta Crystallogr D Biol Crystallogr.* 1998;54(5):905-21.
- 846 33. Zhang Y, Skolnick J. Scoring function for automated assessment of protein structure template
847 quality. *Proteins: Structure, Function, and Bioinformatics.* 2004;57(4):702-10.

- 848 34. Kim DE, Chivian D, Baker D. Protein structure prediction and analysis using the Robetta server.
849 Nucleic Acids Research. 2004 Jul 1;32:W526-W31.
- 850 35. Kelley LA, Mezulis S, Yates CM, Wass MN, Sternberg MJE. The Phyre2 web portal for protein
851 modeling, prediction and analysis. Nature protocols. 2015 Jun;10(6):845-58.
- 852 36. Källberg M, Wang H, Wang S, Peng J, Wang Z, Lu H, et al. Template-based protein structure
853 modeling using the RaptorX web server. Nature protocols. 2012;7(8):1511-22.
- 854 37. Biasini M, Bienert S, Waterhouse A, Arnold K, Studer G, Schmidt T, et al. SWISS-MODEL:
855 modelling protein tertiary and quaternary structure using evolutionary information. Nucleic Acids
856 Research. 2014 Jul 1;42(W1):W252-W8.
- 857 38. Remmert M, Biegert A, Hauser A, Söding J. HHblits: lightning-fast iterative protein sequence
858 searching by HMM-HMM alignment. Nature methods. 2012;9(2):173-5.
- 859 39. Xu JR, Zhang Y. How significant is a protein structure similarity with TM-score=0.5?
860 Bioinformatics. 2010 Apr 1;26(7):889-95.
- 861 40. Wang S, Ma J, Peng J, Xu J. Protein structure alignment beyond spatial proximity. Sci Rep.
862 [Research Support, N.I.H., Extramural
863 Research Support, U.S. Gov't, Non-P.H.S.]. 2013;3:1448.
- 864 41. Zalewski JK, Mo JH, Heber S, Heroux A, Gardner RG, Hildebrand JD, et al. Structure of the
865 Shroom-Rho kinase complex reveals a binding interface with monomeric Shroom that regulates cell
866 morphology and stimulates kinase activity. J Biol Chem. 2016 Oct 10.
- 867 42. Mohan S, Rizaldy R, Das D, Bauer RJ, Heroux A, Trakselis MA, et al. Structure of Shroom
868 domain 2 reveals a three-segmented coiled-coil required for dimerization, Rock binding, and apical
869 constriction. Mol Biol Cell. [Research Support, N.I.H., Extramural Research Support, U.S. Gov't,
870 Non-P.H.S.]. 2012 Jun;23(11):2131-42.
- 871 43. Ioffe S, Szegedy C, editors. Batch Normalization: Accelerating Deep Network Training by
872 Reducing Internal Covariate Shift. Proceedings of The 32nd International Conference on Machine
873 Learning; 2015.
- 874 44. Wang S, Peng J, Ma J, Xu J. Protein secondary structure prediction using deep convolutional
875 neural fields. Sci Rep. 2016;6.
- 876 45. Miyazawa S, Jernigan RL. Estimation of effective interresidue contact energies from protein
877 crystal structures: quasi-chemical approximation. Macromolecules. 1985;18(3):534-52.
- 878 46. Betancourt MR, Thirumalai D. Pair potentials for protein folding: choice of reference states and
879 sensitivity of predicted native states to variations in the interaction schemes. Protein Science.
880 1999;8(02):361-9.
- 881 47. Bergstra J, Breuleux O, Bastien F, Lamblin P, Pascanu R, Desjardins G, et al., editors. Theano: A
882 CPU and GPU math compiler in Python. Proc 9th Python in Science Conf; 2010.
- 883 48. Drozdetskiy A, Cole C, Procter J, Barton GJ. JPred4: a protein secondary structure prediction
884 server. Nucleic acids research. 2015:gkv332.
- 885 49. Wang S, Li W, Liu S, Xu J. RaptorX-Property: a web server for protein structure property

886 prediction. Nucleic acids research. 2016:gkw306.